Adiabatic approximations for the nuclear excitation of molecules by low-energy electron impact: Rotational excitation of H_2

Michael A. Morrison, Andrew N. Feldt, and David Austin*
Department of Physics and Astronomy, The University of Oklahoma, Norman, Oklahoma 73019
(Received 28 March 1983; revised manuscript received 22 September 1983)

The adiabatic-nuclei (AN) theory of nuclear excitation in molecules is critically examined for low-energy e-H_2 collisions in the context of the rigid-rotor approximation. Theoretical concerns relevant to near-threshold scattering processes, where the AN theory is expected to be invalid, are discussed for rotational and vibrational excitation. A quantitative assessment of the AN theory for rotation and of an energy-modified approximation to this theory is obtained by comparison of approximate cross sections to results from laboratory-frame close-coupling calculations. The breakdown of the AN theory for rotation is found to be more severe at energies a few times threshold than was anticipated by rough qualitative arguments made heretofore.

I. INTRODUCTION

Adiabatic approximations abound in physics. In quantum theory, the idea of treating certain relatively slowly varying coordinates as parameters in the study of the other degrees of freedom and subsequently folding in the motion of the slowly varying coordinates via product wave functions is widely used in the study of both bound and continuum states. Thus, the Born-Oppenheimer approximation,[1] in which the nuclear coordinates are treated parametrically, forms the cornerstone of much of the theory of molecular structure and the band theory of solids. In the scattering of charged particles by atoms and molecules, an adiabatic approximation for the coordinates of the scattering particle is used to develop a model of induced-polarization effects.[2]

The most useful implementation of this idea in the quantum theory of electron-molecule scattering is the adiabatic-nuclei (AN) formulation,[3–33] in which the nuclear degrees of freedom of the target are "frozen" during the collision, the nuclear dynamics being taken into account only in the asymptotic region. This formulation is essentially an extension of the Born-Oppenheimer approximation of molecular bound-state theory[1] to the continuum-state problem for the electron-molecule system.[18] Because it allows for a separation of the nuclear and scattering-electron's dynamics, the AN theory has considerable conceptual advantages over a more accurate formulation, such as the laboratory-frame close-coupling (LFCC) theory,[3,34–37] in which the interaction of the motion of the nuclei and that of the scattering electron is fully taken into account. Computationally, such an "exact" treatment is infeasible except for extremely simple systems (e.g., e-H_2).[36,37] The AN theory, although nontrivial to apply to relatively complicated systems, is tractable and consequently has been used to determine cross sections for low- and intermediate-energy nuclear excitations in a huge array of studies that vary widely in their treatment of the collision dynamics and/or of the interaction potential.[38]

The adiabatic approximation was introduced to scattering theory by Chase,[7] who derived approximate expressions for inelastic scattering amplitudes as matrix elements (in the space of the target) of the *elastic* scattering amplitude for *fixed* target coordinates. Oksyuk[8] first particularized Chase's theory to electron-molecule scattering, and Temkin (and co-workers[13–16]) and Hara[10] subsequently developed the AN formulation as it is used today and demonstrated the feasibility of using it to study rotational and vibrational excitation of molecules.

Like all useful approximations, this one runs into trouble in certain circumstances. In particular, the approximations underlying the AN theory are expected to break down for electron collisions with polar molecules,[5] for scattering near a resonance, or for near-threshold excitations. The reasons for the anticipated breakdown have been discussed,[4] and rough qualitative criteria for energies at which it should occur have been articulated.[14] More recently, some attention has been given to formulating alternatives to the AN theory that can be used where it is invalid but which avoid the specter of a full LFCC calculation. Thus, Shugard and Hazi[18] have proposed a modified expression for the inelastic scattering amplitude that requires evaluation of an elastic amplitude off the energy shell, Domcke *et al.*[29] and Nesbet[32] have independently developed nonadiabatic treatments for resonant vibrational excitation, Varracchio[30] has evaluated correction terms to the fixed-nuclei scattering amplitude that incorporate nuclear dynamics, and Norcross and Padial[26] have introduced a modification suitable for electron-polar molecule collisions.

The present paper[39] reports the first detailed quantitative evaluation of the AN theory under conditions where it is expected to break down. In addition to probing the nature and extent of the breakdown of the AN theory, we are investigating alternative formulations for treating collisions under conditions where use of the AN theory is ill-advised; one such alternative, an energy-modified approximation (EMA), is examined herein. An additional long-term goal of this project is the generation of a set of

highly accurate cross sections for very-low-energy nuclear excitations of molecules; such data are essential for applications ranging from analysis of the results of swarm experiments[40] to modeling of planetary atmospheres to understanding the physics of e-beam-initiated gas-discharge lasers.

To accomplish these goals we must use a highly accurate representation of the electron-molecule interaction potential, impose exacting standards of numerical accuracy in the scattering calculations, and, ideally, be able to calculate (or access) benchmark cross sections from a nonadiabatic theory such as LFCC. These requisites can be most fully met for the e-H_2 system, which is the subject of the present inquiry. This system is especially well suited for an investigation of the breakdown of the AN approximation because the nuclear kinetic energy operator is an especially important term in the e-H_2 Hamiltonian; e.g., the spacing of the rotational energy levels in H_2 is on the order of tenths of an eV, rather than, say, 10^{-4}–10^{-5} eV, which is typical of other small molecules. This feature of the target in e-H_2 scattering exacerbates the theoretical deficiencies of the AN theory.

The adiabatic approximation can be applied to the rotational motion, the vibrational motion, or both. Most applications to date have used this theory to study rotational excitation in the rigid-rotator approximation,[4,6] in which the internuclear separation is fixed at its equilibrium value. The resulting adiabatic-nuclear-rotation (ANR) theory is the focus of the calculations presented here. The present paper is, however, the first of a series on nuclear excitations, so the discussions of the theory (Sec. II) and of the model interaction potential (Sec. III) encompass rotational and vibrational degrees of freedom.

In Sec. IV, we briefly describe salient computational details of this work, focusing on problems that arise for near-threshold scattering. Differential and integrated rotational-excitation cross sections from ANR calculations are presented in Sec. V and are compared to those of fully converged LFCC calculations. This section also contains a discussion of the validity of the ANR theory and comments on the EMA and the first Born approximation (FBA). Our conclusions and remarks on the effects of vibrational motion are presented in Sec. VI. Unless otherwise noted, atomic units are used throughout.[41]

II. THEORY

A. Laboratory-frame close coupling

Over 20 years ago, Arthurs and Dalgarno[34] introduced the LFCC theory for the rotational excitation of molecules. This theory has been applied to a few electron-molecule systems[4] and has been extended to incorporate the vibrational degrees of freedom of the nuclei.[37] The LFCC formalism, which fully takes account of the dynamical interaction of the nuclear motion with that of the scattering electron, serves in the present study as the exact theory against which the adiabatic-nuclei and related approximations are assessed. In this subsection, we shall summarize the essential equations and concepts of the LFCC theory.

Since the scattering energies of primary interest in this research are well below the threshold for electronic excitation, we do not allow for such excitation in the theory of this section.[18] (*Virtual* electronic excitations, which correspond to induced polarization of the target,[42] are included approximately, as described in Sec. III D.) Therefore, we begin with the coordinate-space projection of the continuum-state wave function of the system onto the (Born-Oppenheimer) electronic wave function of the $X\,^1\Sigma_g^+$ ground state of H_2. The resulting function depends on the scattering electron's spatial coordinates in the space-fixed reference frame,[43] $\vec{r}'$, and on the coordinates of the internuclear axis $\vec{R}$. It is labeled by the total energy of the system, E, and by the quantum numbers of the initial nuclear target state, which we collectively denote by ν_0. For a linear molecule, $\nu_0=(v_0,j_0,m_{j_0})$, where the quantum numbers v, j, and m_j correspond to the vibrational Hamiltonian $\mathscr{H}_{\rm vib}$, the rotational angular momentum operator $\hat{\vec{j}}^{\,2}$, and the projection of $\hat{\vec{j}}$ on the space-fixed polar (z') axis, respectively.

The "reduced" wave function $\Psi_{E\nu_0}(\vec{r}',\vec{R})$ is an eigenfunction of the effective scattering Hamiltonian

$$\hat{\mathscr{H}}=\hat{T}_e+\hat{\mathscr{H}}^{(n)}+\hat{V}_{\rm int}\ . \tag{1}$$

In space-fixed coordinates, $\hat{T}_e(\vec{r}')$ is the kinetic-energy operator for the scattered electron, $\hat{\mathscr{H}}^{(n)}(\vec{R})$ is the nuclear Hamiltonian of the target, and $\hat{V}_{\rm int}(\vec{r}',\vec{R})$ is the electron-molecule interaction potential averaged over the ground electronic state of the molecule. The nuclear Hamiltonian—in the Born-Oppenheimer approximation[1]—is just the sum of the rotational kinetic-energy operator $\hat{\mathscr{H}}_{\rm rot}(\hat{R})$, the vibrational Hamiltonian $\hat{\mathscr{H}}_{\rm vib}(R)$, and the electronic energy of the ground state. The corresponding nuclear Schrödinger equation determines the target eigenstates $\chi_\nu(\vec{R})$ and the Born-Oppenheimer approximation to the total energy of the molecule in state $\nu=(v,j,m_j)$, ϵ_{vj}, i.e.,

$$\hat{\mathscr{H}}^{(n)}\chi_\nu(\vec{R})=\epsilon_{vj}\chi_\nu(\vec{R})\ . \tag{2}$$

For a diatomic molecule, the target eigenfunctions $\chi_\nu(\vec{R})$ are approximated by products of vibrational and rotational functions (spherical harmonics), viz.,

$$\chi_\nu(\vec{R})=\phi_v(R)Y_{jm_j}(\hat{R})\ , \tag{3}$$

the dependence of the vibrational functions on the rotational quantum number j being neglected.

The interaction potential $\hat{V}_{\rm int}(\vec{r}',\vec{R})$ is, strictly speaking, nonlocal owing to terms arising from antisymmetrization of the electron-molecule system wave function. The nature and treatment of these "exchange terms" has been discussed extensively elsewhere.[44] In the present study they are approximated by local terms; $\hat{V}_{\rm int}$ therefore includes *local* static, exchange, and polarization contributions (see Sec. III).

The total energy of the system—the eigenvalue of $\Psi_{E\nu_0}(\vec{r}',\vec{R})$— is related to the incident and outgoing wave numbers for the excitation $v_0,j_0\rightarrow v,j$ by the energy-

conservation relationship

$$E=\tfrac{1}{2}k_0^2+\epsilon_{v_0j_0}=\tfrac{1}{2}k_{vj}^2+\epsilon_{vj}\ , \tag{4}$$

where $k_0=k_{v_0j_0}$ is the incident wave number.

The LFCC theory (in the coupled-angular-momentum representation[34]) is defined by the laboratory representation—a set of mutually commuting operators the simultaneous eigenfunctions of which constitute the laboratory basis. Introducing $\hat{J}^2$ and $\hat{J}_{z'}$ for the square and z' components of the total angular momentum, we have the laboratory-frame representation:

$$\{\hat{\mathscr{H}}_{\rm vib},\hat{\mathscr{H}}_{\rm rot},\hat{l}^2,\hat{J}^2,\hat{J}_{z'}\}\ . \tag{5}$$

The reduced system wave function appropriate to this representation, $\Psi^{JM}_{Ev_0j_0l_0}(\vec{r}',\vec{R})$, can be expanded in the laboratory basis to obtain the coupled radial differential equations of the LFCC theory. The simultaneous eigenfunctions of the operators in (5) are

$$\Phi^{JM}_{vjl}(\hat{r}',\vec{R})=\phi_v(R)\sum_{m_j,m_l}C(j,l,J;m_j,m_l,M)\times Y_{jm_j}(\hat{R})Y_{lm_l}(\hat{r}')\ , \tag{6}$$

where $C(j_0,l_0,J;m_{j_0},m_{l_0},M)$ is just the appropriate Clebsch-Gordan[45] coefficient. The LFCC expansion

$$\Psi^{JM}_{Ev_0j_0l_0}(\vec{r}',\vec{R})=\frac{1}{r}\sum_{v,j,l}u^J_{vjl,v_0j_0l_0}(r)\Phi^{JM}_{vjl}(\hat{r}',\vec{R}) \tag{7}$$

leads to the coupled radial scattering equations

$$\left[\frac{d^2}{dr^2}-\frac{l(l+1)}{r^2}+\tfrac{1}{2}k_{vj}^2\right]u^J_{vjl,v_0j_0l_0}(r)=\sum_{v',j',l'}V^J_{vjl,v'j'l'}(r)u^J_{v'j'l',v_0j_0l_0}(r)\ . \tag{8}$$

The matrix elements that couple asymptotic channels $(v,j,l;J)$ and $(v',j',l';J)$,

$$V^J_{vjl,v'j'l'}(r)=\langle\Phi^{JM}_{vjl}(\hat{r}',\vec{R})\,|\,V_{\rm int}(\vec{r}',\vec{R})\,|\,\Phi^{JM}_{v'j'l'}(\hat{r}',\vec{R})\rangle\ , \tag{9}$$

are conveniently evaluated by expanding $V_{\rm int}(\vec{r}',\vec{R})$ in Legendre polynomials.[46,47] In terms of the resulting expansion coefficients $v_\lambda(r,R)$, the matrix element (9) becomes

$$V^J_{vjl,v'j'l'}(r)=\sum_\lambda f_\lambda(j,l;j',l';J)\langle\phi_v(R)\,|\,v_\lambda(r,R)\,|\,\phi_{v'}(R)\rangle\ , \tag{10}$$

where the indicated integration is over the coordinate R and where $f_\lambda(j,l;j',l';J)$ are angular-coupling (Percival-Seaton) coefficients.[34] For electron scattering from nonpolar targets, only even non-negative values of λ appear in (10). If the internuclear separation is fixed, say, at its equilibrium value $R=R_{\rm eq}$, as in the rigid-rotor approximation, then the vibrational matrix elements in (10) are replaced by[48] $v_\lambda(r;R_{\rm eq})$.

For convenience, we solve Eqs. (8) subject to the *real* boundary conditions[49]

$$u^J_{v'j'l',v''j''l''}(r)\sim\delta_{v''v'}\delta_{j''j'}\delta_{l''l'}\hat{j}_{l'}(k_{v'j'}r)-\left[\frac{k_{v'j'}}{k_{v''j''}}\right]^{1/2}K^J_{v'j'l',v''j''l''}\hat{n}_{l''}(k_{v''j''}r),\quad \text{as } r\to\infty \tag{11}$$

where $K^J_{v'j'l',v''j''l''}$ is the K matrix element connecting channels $(v',j',l';J)$ and $(v'',j'',l'';J)$. Having obtained the K matrix, the corresponding T matrix can be calculated from

$$\underline{T}=2\underline{K}(\underline{1}-i\underline{K})^{-1} \tag{12a}$$

$$=[2\underline{K}^2(\underline{1}+\underline{K}^2)^{-1}]+i[-2\underline{K}(\underline{1}+\underline{K}^2)^{-1}]\ , \tag{12b}$$

where $\underline{1}$ is the unit matrix. The equivalent form (12b), which explicitly displays the real and imaginary parts of the T matrix, is used in practice (cf. Sec. II C). [The superscript J is left off $\underline{T}$ and $\underline{K}$ in Eqs. (12) because these general relationships also apply to the fixed-nuclei T and K matrices of Sec. II B.]

In discussing approximations to the LFCC formalism, it is useful to relate the T matrix directly to the scattering amplitude. The space-fixed amplitude $f_{vv_0}(\hat{r}')$ is given in terms of LFCC T-matrix elements by[4]

$$f_{vv_0}(\hat{r}')=\frac{2\pi}{(k_0k_{vj})^{1/2}}\sum_{l,m_l}\sum_{l_0,m_{l_0}}\sum_J i^{l_0-l+1}C(j,l,J;m_j,m_l,M)C(j_0,l_0,J;m_{j_0},m_{l_0},M)Y_{lm_l}(\hat{k}'_{vj})Y^*_{l_0m_{l_0}}(\hat{k}'_0)T^J_{vjl,v_0j_0l_0}\ . \tag{13}$$

We shall return to this important relationship in Sec. II D, where it will be used to motivate an approximate alternative to LFCC theory.

Various cross sections can be calculated directly from the T matrix. For example, the integrated rotational-excitation cross section is given by[34]

$$\sigma(v_0,j_0\to v,j)=\frac{\pi}{(2j_0+1)k_0^2}\sum_J(2J+1)\sum_{l,l_0}|\,T^J_{vjl,v_0j_0l_0}\,|^2\ . \tag{14}$$

B. The adiabatic-nuclei theory

The AN theory[3–33] is based on an adiabatic approximation for the nuclear degrees of freedom of the electron-molecule system. In the present application, the nuclear coordinates $\vec{R}$ are regarded as slowly varying, and the scattering electron is described by an adiabatic wave function—the "fixed-nuclei scattering function" of Eq. (17) below. In the AN theory, approximate cross sections for nuclear excitation are determined from matrix elements (in the space of nuclear coordinates) of a fixed-

nuclei transition matrix that is extracted from the adiabatic scattering function. The essential difference, therefore, between the LFCC and the AN theories is in the latter's *approximate* treatment of the dynamical interaction of the motion of the scattering electron and the nuclear degrees of freedom.

A precursor of the AN theory that is important to an understanding of the assumptions on which it is based is the fixed-nuclei (FN) approximation.[9,10] This formulation combines the rigid-rotor and fixed-nuclear-orientation approximations. The latter entails fixing $\hat{R}$ for the duration of the collision; total integrated cross sections (summed over all final rotational states) can subsequently be determined[4] by averaging fixed-nuclear-orientation scattering quantities over $\hat{R}$. Fixed-nuclei calculations are most conveniently carried out in a body-fixed reference frame, as described below. In terms of the Hamiltonian (1), the FN approximation amounts to total neglect of the nuclear Hamiltonian, which, in the rigid-rotor approximation, is just $\mathscr{H}_{\rm rot}$.

The nuclear Hamiltonian is partly taken into account in the AN theory. In particular, the perturbation of the scattering function by $\hat{\mathscr{H}}^{(n)}$ and the energy separation between target states are ignored in the calculation of the FN scattering matrix. These aspects of the collision physics are introduced approximately via appropriate unitary transformations that yield an S matrix in a basis in which the target states are properly treated as nondegenerate.

Considerable insight into the question of the validity of the AN theory can be gained by adopting the viewpoint of the frame-transformation theory of Chang and Fano.[50] These authors pointed out that formally the validity of this theory hinges on the commutator $[\hat{\mathscr{H}}^{(n)},\hat{V}_{\rm int}]$ being small—a condition that emphasizes the importance of the representation of the interaction potential used in scattering calculations (cf. Sec. V B 3). Conceptually, neglect of $\hat{\mathscr{H}}^{(n)}$ in the determination of the adiabatic scattering function would seem to be a reasonable approximation if most of the distortion of that function occurs near the target, where the Coulomb interactions predominate. This criterion leads us to expect the AN theory to be reliable if the scattering energy is large—say, compared to the expectation value of $\hat{\mathscr{H}}^{(n)}$ for the target states of interest. Such is not the case near threshold.

The scattered electron that emerges from a near-threshold nuclear excitation has very little kinetic energy, and the corresponding scattering function will be very sensitive to the region far from the target, where the nuclear Hamiltonian may be a significant perturbative influence. If so, the AN theory will be unable to predict correct inelastic cross sections. Moreover, near-threshold scattering energies will be comparable to the energy spacing between the initial and final nuclear target states, which, in the AN theory, are treated as degenerate.

The inaccuracy of the assumption of target-state degeneracy is strikingly manifested in the AN differential cross sections, which, in violation of the Wigner threshold laws,[51] do not vanish at threshold. Chang and Temkin[11] introduced an *ad hoc* remedy for this undesirable behavior by simply multiplying the AN cross section for nuclear excitation $v_0 j_0 \rightarrow vj$ by the wave-number ratio k_{vj}/k_0. (This modification is used in all the AN calculations reported in this paper.) The resulting AN inelastic cross sections do not, however, exhibit the proper dependence on k_{vj} near threshold (see Sec. II C).

In the remainder of this section, we briefly survey the AN formulation. Although the results in Sec. V pertain to the *rotational* degrees of freedom only, we shall, for completeness, include in the theoretical discussion the vibrational degrees of freedom as well.

In the AN formulation, the scattering equations are written in a body-fixed (BF) reference frame. The BF axes are obtained from the space-fixed (SF) axes by a rotation through the Euler angles chosen to align the BF polar axis with the internuclear axis, which will be fixed throughout the collision. The spatial coordinates of the scattering electron in the BF reference frame will be unprimed[43] ($\vec{r}$).

In contrast to the laboratory-frame representation (5), the AN theory is formulated in terms of the body-frame representation

$$\{\hat{\mathscr{H}}_{\rm vib},\hat{l}^2,\hat{\vec{l}}\cdot\hat{R},\hat{J}^2,\hat{\vec{J}}\cdot\hat{R},\hat{J}_{z'}\}\ , \tag{15}$$

where $(\hat{\vec{l}}\cdot\hat{R})$ is the projection of $\hat{\vec{l}}$ on the internuclear axis. The corresponding quantum numbers[52] v, l, Λ, J, Λ, and M label the asymptotic free body-frame states and the body-frame basis functions,

$$\chi^{JM}_{vl\Lambda}(\hat{r},\vec{R})=\phi_v(R)Y_{l\Lambda}(\hat{r})R_{JM\Lambda}(\hat{R})\ . \tag{16}$$

The rotational functions $R_{JM\Lambda}(\hat{R})$ in (16) are those of the symmetric top.[45,53]

For the reduced wave function in the AN formulation we choose a function with initial-channel labels that are consonant with the body-frame representation (15). Letting E_b denote the body-frame energy (the scattering energy at which the BF-FN scattering matrix is evaluated), we represent this wave function by $\Gamma^{JM}_{E_b v_0 l_0 \Lambda}(\vec{r},\vec{R})$.

Invoking the adiabatic approximation, we replace the system wave function by the product of the adiabatic (FN) scattering function $\Omega^{\Lambda}_{E_b l_0}(\vec{r};R)$ and the initial-channel nuclear target function, viz.,

$$\Gamma^{JM}_{E_b v_0 l_0 \Lambda}(\vec{r},\vec{R})\simeq\Omega^{\Lambda}_{E_b l_0}(\vec{r};R)[\phi_{v_0}(R)R_{JM\Lambda}(\hat{R})]\ , \tag{17}$$

where the semicolon indicates the *parametric* dependence of $\Omega^{\Lambda}_{E_b l_0}$ on R. From the asymptotic behavior of $\Omega^{\Lambda}_{E_b l_0}(\vec{r};R)$ we can obtain BF-FN scattering matrices.

The BF-FN radial scattering functions that yield the K matrix, $w^{\Lambda}_{ll_0}(r;R)$, are introduced via a partial-wave expansion of $\Omega^{\Lambda}_{E_b l_0}(\vec{r};R)$ in a basis of BF spherical harmonics $\{Y_{l\Lambda}(\hat{r})\}$. The resulting BF-FN coupled equations have the form

$$\left[\frac{d^2}{dr^2}-\frac{l(l+1)}{r^2}+k_0^2\right]w^{\Lambda}_{ll_0}(r;R) =2\sum_{l'}V^{(\Lambda)}_{ll'}(r;R)w^{\Lambda}_{l'l_0}(r;R)\ . \tag{18}$$

The coupling matrix elements in (18) are conveniently

evaluated (at internuclear separation R) in terms of the Legendre expansion coefficients $v_\lambda(r,R)$ as

$$V_{ll'}^{(\Lambda)}(r;R)=\sum_\lambda g_\lambda(l,l';\Lambda)v_\lambda(r;R)\ , \tag{19}$$

where the angular-coupling coefficients are

$$g_\lambda(l,l';\Lambda)=(-1)^\Lambda\frac{[(2l+1)(2l'+1)]^{1/2}}{2\lambda+1}\times C(l,l'\lambda;0,0,0)C(l,l'\lambda;-\Lambda,\Lambda,0)\ . \tag{20}$$

The BF-FN K matrix $\underline{K}^\Lambda(R)$ is obtained by imposing on the solutions of (18) the boundary conditions

$$w_{ll_0}^\Lambda(r;R)\sim\delta_{ll_0}\hat{j}_{l_0}(k_br)-K_{ll_0}^\Lambda(R)\hat{n}_l(k_br),\ \text{as } r\to\infty \tag{21}$$

and the corresponding T matrix $\underline{T}^\Lambda(R)$ is then determined by using $\underline{K}^\Lambda(R)$ for $\underline{K}$ in Eqs. (12).

To obtain, from the BF-FN T matrix, the AN approximation to inelastic cross sections, we must introduce the unitary transformations[54,55] that affect the necessary coordinate rotation and change of representation[4,50] to produce an approximate LF T matrix, i.e., one that connects states defined in the representation (5), $|E_b,v_0,j_0,l_0,J,M\rangle$ and $|E_bvjlJM\rangle$. The vibrational degrees of freedom are introduced asymptotically via the vibrational frame transformation,

$$T_{vl,v_0l_0}^\Lambda=\langle\phi_v(R)\,|\,T_{ll_0}^\Lambda(R)\,|\,\phi_{v_0}(R)\rangle\ . \tag{22}$$

(In the ANR theory, which is examined in Sec. V, this step is by-passed since the rigid-rotor approximation fixes R at its equilibrium value.)

The rotational degrees of freedom are introduced via the rotational frame transformation,[50] which relates simultaneous eigenfunctions of the laboratory-frame representation (5) in SF coordinates to those of the body-frame representation (15) in BF coordinates. The AN approximation to the LF T matrix $\underline{T}^J$ has elements

$$\mathscr{T}_{vjl,v_0j_0l_0}^J=\sum_\Lambda A_{j\Lambda}^{Jl}\langle\phi_v(R)\,|\,T_{ll_0}^\Lambda(R)\,|\,\phi_{v_0}(R)\rangle A_{j_0\Lambda}^{Jl_0}\ , \tag{23}$$

where $\underline{A}$ is the transformation matrix[4]

$$A_{j\Lambda}^{Jl}=\left[\frac{2j+1}{2J+1}\right]^{1/2}C(j,l,J;0,\Lambda,\Lambda)\ . \tag{24}$$

These matrix elements can be used in the appropriate LFCC formulas[34] to calculate AN approximations to differential and integrated cross sections for nuclear excitations at body-frame energy E_b.

The rotational frame transformation (24) can also be used to relate the coordinate-space projections of the body- and laboratory-frame scattering functions, viz.,

$$\Psi_{E_bv_0j_0l_0}^{JM}(\vec{r}',\vec{R})=\sum_\Lambda A_{j_0\Lambda}^{Jl_0}\Gamma_{E_bv_0l_0\Lambda}^{JM}(\vec{r},\vec{R})\ . \tag{25}$$

The essential ambiguity of the AN theory and the major source of concern at the prospect of using it for near-threshold collisions rests in the definition of the body-frame energy. In his seminal paper on the use of the adiabatic approximation for scattering processes, Chase[7] picks E_b to be the scattering energy relative to the *initial* target state, $\frac{1}{2}k_0^2$ [cf. Eq. (4)]; this choice has been used in nearly all implementations of AN theory and is the one chosen for the ANR study reported in Sec. V. Chang and Temkin[14] propose the alternative choice $E_b=\frac{1}{2}k_{vj}^2$ as desirable for scattering calculations near the threshold for the excitation $(v_0j_0)\to(vj)$. But, as discussed by Shugard and Hazi[18] and by Norcross and Padial,[26] *rigorous* identification of E_b within the AN formalism is impossible. This ambiguity is a consequence of the assumed degeneracy of the nuclear target states in this theory. For scattering energies well above threshold, this ambiguity need not concern us, and the choice $E_b=\frac{1}{2}k_0^2$ is reasonable. However, near threshold this choice introduces significant error in the AN cross sections (cf. Sec. V).

The origin of this error can be clearly seen by examining the AN approximation to the laboratory-frame (LF) scattering amplitude,[4]

$$f_{v_0}(\hat{r}')=f(k_b\hat{r}',\ v\leftarrow\vec{k}_b',v_0)=\frac{2\pi}{k_b}\sum_{l,m_l}\sum_{l_0,m_{l_0}}\sum_J i^{l_0-l+1}C(j,l,J;m_j,m_l,M)C(j_0,l_0,J;m_{j_0},m_{l_0},M)Y_{lm_l}(\hat{r}')Y_{l_0m_{l_0}}^*(\hat{k}_b')\mathscr{T}_{vjl,v_0j_0l_0}^J\ . \tag{26}$$

In this expression k_b is the body wave number $k_b=\sqrt{2E_b}$; this value therefore corresponds to the energy at which $\underline{T}^\Lambda(R)$ and hence $\underline{\mathscr{T}}^J$ is evaluated. Equation (26) is the AN counterpart of (13) for the exact LFCC scattering amplitude. Comparison of these two expressions reveals that structurally the only difference is the replacement of k_b in the prefactor in (26) by $(k_{vj}k_0)^{1/2}$ in the exact result. The conventional choice $k_b=k_0$ clearly does not lead to an approximate scattering amplitude with the correct dependence on k_{vj} near threshold.

C. Threshold laws

The threshold laws for the LFCC and AN T matrices are of great importance to an understanding of the breakdown of the AN theory for near-threshold nuclear excitations. The threshold behavior of the scattering matrix is a familiar topic in collision theory.[51,56–58] In this section the analysis of Bardsley and Nesbet[56] for multichannel electron-atom scattering is extended to rovibrational electron-molecule scattering. (The threshold behavior of the BF-FN K matrix has been studied from the viewpoint

of effective-range theory by Fabrikant.[58])

Near-threshold excitations are caused primarily by the long-range part of the interaction potential.[4,59,60] For electron-molecule scattering, this part consists of terms due to permanent (static) and induced moments. The elements of the T matrix vanish at threshold and are small in the energy region of interest. Their dependence on wave number can therefore be determined from the first term in the Born Series for $\underline{T}$, i.e., in the FBA.

The FBA is used in the Appendix to obtain analytic expressions for the LFCC and AN T matrices $\underline{T}^J$ and $\underline{\mathscr{T}}^J$ at energies near threshold. All results in the present discussion follow from the indicated equations in the Appendix. [Since, in the FBA, the T and K matrices are proportional ($\underline{T}=-2i\underline{K}$), the following results also describe the threshold behavior of the K matrix.]

The dependence of the LFCC T-matrix elements on the outgoing-electron wave number follows from the FBA result (A5) and the behavior of the radial integral (A8) as $k_{vj}/k_0\to 0$, viz.,

$$T^J_{vjl,v_0j_0l_0}\sim k_{vj}^{l+1/2},\quad \text{as } k_{vj}\to 0\ . \tag{27}$$

Interestingly, this threshold law turns out to be identical to that obtained if the interaction is assumed to be short range, i.e., $v_\lambda(r,R)\simeq 0$ for $r>r_{\max}$ for all λ. Thus we find that in the LFCC formulation, the presence of long-range interactions does not affect the threshold law. This result, which is the same as that discovered by Bardsley and Nesbet[56] for inelastic electron-atom scattering, does *not* obtain in the AN formulation.

The threshold law for the frame-transformed matrix element $\mathscr{T}^J_{vjl,v_0j_0l_0}$ follows directly from the FBA expression for the BF-FN matrix element $T^\Lambda_{ll_0}(R)$, since the unitary transformations that relate these matrix elements [cf. Eq. (23)] are independent of energy. For a long-range potential energy of the form $r^{-s_\lambda}P_\lambda(\cos\theta)$, we find [from (A14) and the radial integral (A17)] that in the FBA, $T^\Lambda_{ll_0}$ is proportional to $k_b^{s_\lambda-2}$ and, hence, that the threshold law in the AN theory is[60]

$$\mathscr{T}^J_{vjl,v_0j_0l_0}\sim k_b^{s_\lambda-2},\quad \text{as } k_b\to 0\ . \tag{28}$$

For example, for the $s_\lambda=3$ quadrupole interaction, the T-matrix elements are proportional to k_b, while for the $s_\lambda=4$ induced-polarization interaction, Eq. (28) predicts a k_b^2 dependence. The appearance of the body-frame wave number k_b in the threshold law brings us back to the essential ambiguity of the AN theory, namely, the definition of this quantity.

Regardless of how one chooses k_b, the threshold behavior of the LFCC and AN T matrices differs in several respects. For example, unlike the LFCC law (27), the AN law (28) applies only to long-range potentials. [If one assumes a short-range interaction, then the radial integral (A16) is proportional to $k_b^{l_0+l}$, and $\mathscr{T}^J_{vjl,v_0j_0l_0}$ exhibits a $k_b^{l_0+l+1}$ dependence on the body-frame wave number, in contrast to (28), which is independent of l.]

This observation illustrates the fact that invoking the FBA in the LFCC and AN theories leads to distinctly different results for the T matrix. (This conclusion may be germane to theoretical treatments in which the LFCC and AN theories are mixed[26] and the FBA is used.) Insight into these differences can be gained by examining the ratio of corresponding FBA T matrix elements for a quadrupole potential; for $l=l_0\neq 0$, we obtain

$$\frac{T^J_{vjl,v_0j_0l_0}}{\mathscr{T}^J_{vjl,v_0j_0l_0}}\sim\frac{k_b}{k_0}\left[\frac{k_0}{k_{vj}}\right]^{l_0+1/2}\frac{2}{\sqrt{\pi}}\frac{\Gamma(l_0+\frac{3}{2})}{\Gamma(l_0+2)}\ ,$$

$$\text{as } k_{vj}\to 0\ . \tag{29}$$

where $\Gamma(x)$ is the gamma function.[61] In the conventional application of AN theory, with $k_b=k_0$, the ratio (29) is proportional to $k_{vj}^{-(l_0+1/2)}$, which certainly does not approach unity as $k_{vj}\to 0$. Even in the EMA, which is discussed in Sec. II D, the ratio of exact to approximate T-matrix elements does not go to 1. (Further discussion of the use of the FBA for very-low-energy inelastic electron-molecule scattering will be found in Sec. V C.)

The main results of this section, Eqs. (27) and (28), explicitly show the inadequacy of conventional AN theory—in which $\mathscr{T}^J_{vjl,v_0j_0l_0}$ is independent of k_{vj}—to properly describe near-threshold electron-molecule collisions. The alternative proposed by Chang and Temkin,[14] $k_b=k_{vj}$, is an improvement on the conventional choice $k_b=k_0$ only in that it forces $\mathscr{T}^J_{vjl,v_0j_0l_0}$ to go to zero at threshold.

D. An energy-modified approximation

In light of the breakdown of conventional AN theory for certain scattering processes, some theorists have proposed alternative approaches that seek to incorporate nonadiabatic effects without introducing the computational difficulties of a full LFCC calculation.[26,29–32] One such proposal was made by Nesbet[32] in a recent paper in which the formal relationship between the LFCC and AN theories was elucidated. The emphasis in this paper was on resonant vibrational excitation (in e-N_2 collisions) and hence on the adiabatic approximation for vibration. The central result of Nesbet's analysis was the demonstration that replacement of the body-frame energy E_b in the BF-FN scattering equations with the operator $E-\hat{\mathscr{H}}^{(n)}$ leads to an equation that is formally equivalent to the scattering equation of LFCC theory. Therefore, the FN scattering matrix properly should depend on the kinetic energy of the nuclear motion.

Nesbet's EMA is an improvement on the AN theory of Sec. II in that it approximately incorporates this dependence, which is especially important near threshold. The EMA is designed to ensure proper behavior of each element of the S matrix as the energy approaches threshold and to guarantee unitarity of the S matrix. To enforce the latter condition,[62] the EMA is formulated in terms of the K matrix, which is explicitly constructed so as to be symmetric.

The essential idea of Nesbet's EMA, generalized to the present context, in which the rotational and vibrational degrees of freedom are treated adiabatically, is the deter-

mination of the approximate K-matrix element $\mathscr{K}^J_{v'j'l',v''j''l''}$ by frame-transforming the BF-FN K matrix $\underline{K}^\Lambda(R)$ via an equation analogous to (23), the latter having been calculated at a body energy equal to the *geometric mean* of the initial- and final-state scattering energies *for this element*, i.e., at

$$E_b = \tfrac{1}{2} k_{v'j'} k_{v''j''} . \tag{30}$$

The EMA T matrix $\underline{\mathscr{T}}^J$ is then obtained by substituting the EMA $\underline{\mathscr{K}}^J$ into Eqs. (12).

This strategy has several advantages over the AN theory of Sec. II B. Most important, it leads to approximate scattering matrices that *do* depend on the nuclear dynamics. Thus, each element of the EMA T matrix goes to zero at the appropriate threshold ($k_{vj} \to 0$). Second, it prescribes that the diagonal elements of $\underline{\mathscr{K}}^J$ are to be evaluated at the appropriate channel energy, $k^2_{v'j'} = 2(E - \epsilon_{v'j'})$ [cf. Eq. (4)]. Finally, it guarantees that certain crucial T-matrix elements will obey the LFCC threshold law (27).

Near threshold, where $\mathscr{T}^J_{vjl,v_0j_0l_0}$ is proportional to $\mathscr{K}^J_{vjl,v_0j_0l_0}$, the EMA prescription leads to approximate T-matrix elements that obey (28) with $k_b = (k_0 k_{vj})^{1/2}$; taking $s_\lambda = 3$ for the (dominant) quadrupole interaction, we find the EMA threshold law

$$\mathscr{T}^J_{vjl,v_0j_0l_0} \sim k_{vj}^{1/2}, \quad \text{as } k_{vj} \to 0 . \tag{31}$$

Therefore each element of $\underline{\mathscr{T}}^J$ for which $l = 0$ (outgoing s wave) has the correct threshold behavior (27). This feature is especially important for rotational excitations with $\Delta j = 2$; at near-threshold energies, LFCC cross sections for this process are predominantly determined[36] by the $l = 0$, $l_0 = 2$ elements of $\underline{T}^J$. These crucial elements of the EMA T matrix exhibit the threshold law (31) rather than the AN law (28).

The comparison of the LFCC and EMA threshold laws reveals one of the disadvantages of this procedure: All elements of the EMA T matrix with $l > 0$ *do not* have the proper near-threshold dependence on k_{vj}. For example, one need not go far above the threshold for a $\Delta j = 2$ rotational excitation before the $l = l_0 = 1$ elements of $\underline{T}^J$ make the dominant contribution to the inelastic cross section. [For e-H_2 scattering with the interaction potential described in Sec. III, 85% of the LFCC cross section $\sigma(0 \to 2)$ at a scattering energy of 0.047 eV comes from the $d \to s$ T-matrix element, while at 0.08 eV this cross section is a mixture of contributions: 27% from $d \to s$ elements and 59% from $p \to p$ elements.] The EMA T-matrix elements for $l = 1$ exhibit the threshold behavior of Eq. (31), rather than the $k_{vj}^{3/2}$ dependence required by (27). The importance of this defect in the EMA T matrix is mitigated somewhat for $\Delta j = 2$ cross sections because of the aforementioned dominance of $l = 0$ elements in their determination.

A more practical disadvantage of this EMA prescription derives from the nature of Eqs. (12), which are used to obtain $\underline{\mathscr{T}}^J$. To calculate the cross section for the particular excitation $v_0, j_0 \to v, j$, we require T-matrix elements $\mathscr{T}^J_{vjl,v_0j_0l_0}$ for a range of values of l, l_0, and J. Except *very* near threshold, where the FBA provides a one-to-one correspondence between $\mathscr{K}^J_{vjl,v_0j_0l_0}$ and $\mathscr{T}^J_{vjl,v_0j_0l_0}$ determination of the necessary T-matrix elements requires knowledge of K-matrix elements $\mathscr{K}^J_{v'j'l',v''j''l''}$ for a large number of values of v', j' and v'', j'' (including, of course, $v', j' = v, j$ and $v'', j'' = v_0, j_0$). This fact means that we must solve the BF-FN scattering equations for $\underline{K}^\Lambda(R)$ at several body energies (30) and assemble $\underline{\mathscr{K}}^J$ by frame-transforming all these submatrices. The need for several BF-FN calculations to study a given nuclear excitation via the EMA markedly increases the requisite computer time.

Several routes around this difficulty come to mind. For example, one could initially generate $\underline{K}^\Lambda(R)$ over a mesh of energies and use an interpolation scheme to obtain the K-matrix elements needed for a particular inelastic cross section. This tactic may be perilous because of the occasionally strong dependence of $\underline{K}^\Lambda(R)$ on k_b. Alternatively, one could deal directly with the T matrix, evaluating $\underline{T}^\Lambda(R)$ at $k_b = (k_0 k_{vj})^{1/2}$ and proceeding directly—via the frame-transformation (23)—to the elements of $\underline{\mathscr{T}}^J$ needed to compute $v_0, j_0 \to v, j$ cross sections. However, this tactic sacrifices unitarity of the S matrix and the computational convenience of imposing real (K-matrix) rather than complex (S-matrix) boundary conditions in solving the BF-FN coupled equations.

We have implemented a simpler modification to the original EMA procedure, taking a hint from comparison of the LFCC and AN expressions for the LF scattering amplitude for the excitation of interest, Eqs. (13) and (26), respectively. Noting that replacing k_b, the wave number at which $\underline{\mathscr{T}}^J$ in (26) is evaluated, by the geometric mean of the wave numbers for the excitation $v_0 j_0 \to vj$, $(k_0 k_{vj})^{1/2}$, makes (26) identical in form to (13), we evaluate the full matrix $\underline{\mathscr{T}}^J$ from the BF-FN T matrix $\underline{T}^\Lambda(R)$ at body wave number $k_b = (k_0 k_{vj})^{1/2}$. This matrix is obtained via Eq. (12) from $\underline{K}^\Lambda(R)$, which is extracted from the asymptotic behavior of the solution matrix of Eq. (18) at the corresponding body-frame energy. Thus, in our implementation, only one BF-FN scattering calculation is required to study a particular scattering process.

This modified EMA sacrifices unitarity of the S matrix for the sake of computer-time considerations. Its implementation is quite straightforward, and it shares with the original EMA procedure the desirable threshold law (31) for the crucial T-matrix elements for the $v_0, j_0 \to v, j$ cross section. (It also shares the less desirable behavior for $l > 0$ elements. In another paper,[63] we have reported a new "scaled AN theory" that avoids this defect.) Finally, it yields cross sections $\sigma(j_0, v_0 \to j, v)$ that go to zero as $k_{vj} \to 0$ and hence obviates the need for multiplication of the approximate cross sections by the *ad hoc* wave-number ratio k_{vj}/k_0 of Chang and Temkin.[11]

III. THE INTERACTION POTENTIAL

The construction of an accurate interaction potential is as important to the calculation of cross sections for low-energy electron-molecule collisions as the formulation of the scattering theory. The complexity of the system prohibits an exact treatment of the particle-target interaction, but research in this field has demonstrated that reli-

able cross sections can be determined using model potentials.[44,64] Any credible electron-molecule interaction potential (for low-energy scattering) must take account of electrostatic, exchange, and induced-polarization effects, viz.,

$$V_{\rm int}(\vec{r},R)=V_{\rm st}(\vec{r},R)+V_{\rm ex}(\vec{r},R)+V_{\rm pol}(\vec{r},R)\ . \qquad (32)$$

The accuracy of the model potential is of particular concern in the present context because formally the validity of the AN theory depends explicitly on $V_{\rm int}$ (cf. Sec. II B). A second consideration is that this potential be free of parameters that must be determined by appeal to experimentally measured cross sections. Finally, we want a procedure that can easily and consistently be extended to nonequilibrium internuclear separations.

In this section we describe briefly the treatments we have adopted for each of the components of $V_{\rm int}$ in (32), beginning with the wave function used to represent the ground electron state of the target. This function is used in determining all parts of $V_{\rm int}$.

A. Basis set for H_2

In order to implement the LFCC and AN theories for rovibrational excitation, we require near-Hartree-Fock electronic wave functions[65] for the $X\,^1\Sigma_g^+$ state of H_2 for a range of internuclear separations. We determined these functions using a POLYATOM computer package,[66] which carries out self-consistent-field (linear-variational) calculations using a basis comprised of nucleus-centered Gaussian-type orbitals. We used an extended basis set containing contracted functions for the $1\sigma_g$ molecular orbital of H_2 and two p-type polarization functions (with exponents of 2.228 and 0.5183). To assess the quality of the resulting electronic function, it is useful to examine the electronic energy and the quadrupole moment.

At $R=1.402a_0$, our basis yields an electronic energy of $-1.132\,895E_h$. The Hartree-Fock limit for this geometry[67] is $-1.133\,63E_h$. The highly accurate configuration-interaction calculations of Kolos and Wolniewicz[68] yield the value $-1.174\,47E_h$.

Because of the role played by the electron-quadrupole interaction in rotational excitation, the quadrupole moment of the molecule $q(R)$ is of particular importance. At $1.4a_0$, our electronic function produces $q(R)=0.4518ea_0^2$. This result compares favorably with the experimental value[69–71] of $(0.474\pm0.034)ea_0^2$, which, of course, includes averaging over the vibrational motion of the nuclei,[72] and with the $R=1.4a_0$ value $0.4568ea_0^2$ obtained from configuration-interaction calculations by Poll and Wolniewicz.[73]

B. The static potential

The most important component of the interaction potential is the static term, $V_{\rm st}(\vec{r},R)$ in (32). This contribution originates in the Coulomb interactions between the scattering electron and the constituent electrons and nuclei of the target. In the formulation of Sec. II, this potential results from averaging the Coulomb potential energy over the $X\,^1\Sigma_g^+$ wave function described in Sec. III A.

The interaction potential appears in the single-center theory of Sec. II buried in the coupling matrix elements [(10) for the LFCC theory, (19) for the AN formulation] as the Legendre coefficients $v_\lambda(r,R)$. Each static coefficient $v_\lambda^{\rm st}(r,R)$ is the sum of electron-nucleus and electron-electron terms;[74] the latter must be evaluated from the neutral probability density.

The calculation of $v_\lambda^{\rm st}(r,R)$ from the electronic function of Sec. III A was carried out using the programs ALAM (Ref. 46) and VLAM (Ref. 47). Four such terms ($\lambda=0,2,4,6$) were sufficient to obtain fully converged cross sections for e-H_2 scattering at energies up to 13 eV.

C. Exchange

In the scattering theory of Sec. II we did not explicitly impose the antisymmetrization requirement of the Pauli principle on the system wave function, since doing so would lead to coupled *integro-differential* radial scattering equations,[44] the solution of which is computationally quite arduous—if, indeed, it is possible at all. This difficulty is especially acute for vibrational-excitation studies and for calculations on complex molecules, both of which are long-term objectives of this program. Therefore we have used an approximate treatment of exchange effects that markedly simplifies the computations.

Research on such treatments in recent years has demonstrated their utility in reliably mocking exchange effects via a *local* potential-energy term[44] that can be simply added to $V_{\rm st}(\vec{r},R)$. Although our model-exchange potential was determined in a BF-FN study (described below), it is used in the LFCC and AN calculations reported in Sec. V.

The particular model-exchange potential we used is a variant of the free-electron-gas (FEG) potential originally proposed by Hara[75] as an extension to scattering problems of Slater's average exchange potential for bound states. Extensive discussions of the theory underlying this model, of its relation to an exact treatment of exchange, and of its accuracy for electron-molecule scattering can be found elsewhere.[76] Briefly, we note that the form of the potential derives from making two approximations in the integral exchange terms of the exact-exchange scattering equations. First, the molecular electrons are treated as a FEG, with a charge density $\rho(\vec{r},R)$ determined from the ground-state electronic function of the target (cf. Sec. III A). Second, the distortion of the continuum function is neglected. The resulting FEG exchange potential has the form

$$V_{\rm ex}(\vec{r},R)=-\frac{2}{\pi}k_F(\vec{r};R)\left[\frac{1}{2}+\frac{1-\eta^2}{4\eta}\ln\left|\frac{1+\eta}{1-\eta}\right|\right], \qquad (33)$$

where $k_F(\vec{r};R)=[3\pi^2\rho(\vec{r};R)]^{1/3}$ is the Fermi momentum and $\eta=\kappa/k_F$. The local momentum κ is defined as

$$\kappa(\vec{r})=[2(E_{\rm inc}+I)+k_F^2(\vec{r},R)]^{1/2}\ . \qquad (34)$$

In LFCC calculations, the incident energy E_{inc} in (34) is the initial-channel energy $\frac{1}{2}k_0^2$. In BF-FN calculations for AN or EMA studies, E_{inc} is the body energy E_b. In Hara's FEG potential,[75] I in (34) is the ionization potential of the neutral target. Legendre expansion coefficients of $V_{ex}(\vec{r},R)$ can be calculated using the program EXLAM (Ref. 77) and simply added to the static coefficients discussed in Sec. III B.

This potential has been shown to be a rather accurate approximation for electron scattering from a wide variety of many-electron molecules.[44] For systems in which the target has few electrons (e.g., H_2), Hara's potential is less successful,[44,76] probably due to inadequacy of the FEG approximation for such a molecule. However, an exchange potential of the form of (33) can be used for such systems provided I in (34) is treated as a parameter.[76] Gibson and Morrison[78] showed that the resulting "tuned free-electron-gas exchange" (TFEGE) potential gives accurate total integrated and differential cross sections for e-H_2 scattering over three decades of energy. In the present study, we used a *newly determined* TFEGE potential.

The tuning procedure is carried out in the BF-FN formulation within the static-exchange approximation, in which induced-polarization effects are neglected (cf. Sec. III D). This procedure requires knowledge of the eigenphase sum[79] in *one* symmetry at *one* energy from an exact-static-exchange (ESE) calculation, in which the integro-differential BF-FN radial scattering equations are solved. The parameter I in (34) can then be adjusted so that corresponding static-model-exchange calculations, in which the exchange potential (33) is simply added to $V_{st}(\vec{r},R)$, yield the *same* value of the eigenphase sum. This tuning fully determines $V_{ex}(\vec{r},R)$ at each R; no further adjustments are made.

In our original report on the ANR theory,[39] we showed results obtained with a TFEGE potential that was obtained by tuning in the Σ_g symmetry. Study of the matrix elements (19) reveals that doing so amounts to adjusting primarily the *spherical* component of the exchange potential, $v_0^{ex}(r,R)$. This component plays an important role in determining total and elastic cross sections because it "connects" channels with $l=l_0$. For example, these "s-wave" T-matrix elements (with $J=0$) make the most important contribution to $\sigma(j_0\rightarrow j_0)$ in Eq. (14). In the BF-FN formalism, s waves are present only in the Σ_g symmetry, so tuning in this symmetry is the optimum choice for calculations the primary focus of which is the total (or elastic) cross section.

This choice is less shrewd for the study of rotational excitation because of the importance of the nonspherical components of V_{int} in the determination of cross sections for this collision process (e.g., $\lambda=2$ for $\Delta j=2$ excitations). A preferable alternative is the Σ_u symmetry; tuning in this symmetry entails adjusting $v_0^{ex}(r,R)$ and $v_2^{ex}(r,R)$. Moreover, p waves ($l=1$) are present in the Σ_u scattering equations, which, unlike those of the Σ_g symmetry, contain odd-order partial waves. Rotational- and vibrational-excitation cross sections are strongly influenced by these partial waves. [For example, for scattering energies above 65 meV, the $J=l=l_0=1$ T-matrix elements make important contributions to $\sigma(0\rightarrow 2)$ in Eq. (14).]

Hence we redetermined the TFEGE for the present study by tuning Eq. (33) in the Σ_u symmetry. The tuning energy was $E_b=0.04$ Ry$=0.544$ eV, which is just above the threshold for the $v_0=0\rightarrow v=1$ excitation.

To ensure internal consistency, we first performed new ESE calculations using the H_2 ground-state electronic function described in Sec. III A. Using the iterative static-exchange method of Collins *et al.*,[80] we solved the BF-FN integro-differential equations in the Σ_u (and Σ_g) symmetries, obtaining the eigenphase sums shown in Table I. The choice $I=3.797$ eV in Eq. (34) was found to give a static-model exchange Σ_u eigenphase sum at 0.04 Ry of 0.0487 rad, which agrees with the corresponding ESE value. This value of I is larger than the one obtained when the tuning is performed in the Σ_g symmetry at the same energy ($I=1.787$ eV) and yields a less attractive FEG exchange potential.

The effect on the static-exchange eigenphase sums and on rotational-excitation cross sections of alternate choices of the TFEGE potential is relevant to the overall credibility of the cross sections in Sec. V. In Table I, we present static-model-exchange eigenphase sums in the Σ_g and Σ_u symmetries calculated with both model potentials. Examination of these results shows that the deviation of these approximate results from their ESE counterparts, while quite small near the tuning energy, increases with increasing E_b.

Table I provides an indication of the accuracy of our

TABLE I. BF-FN ($R=1.4a_0$) static-exchange eigenphase sums (in radians) for e-H_2 scattering from ESE and model-exchange ("tuned") calculations. In the latter the TFEGE of Eq. (33) was used with I in Eq. (34) chosen to ensure agreement with the ESE eigenphase sum at 0.04 Ry in either the Σ_g or Σ_u symmetry. All calculations use the basis described in Sec. III A.

	Σ_g eigenphase sum			Σ_u eigenphase sum		
E_b (Ry)	ESE	Σ_g-tuned[a]	Σ_u-tuned[b]	ESE	Σ_g-tuned[a]	Σ_u-tuned[b]
0.01	2.9307	2.9327	2.9181	0.0135	0.0153	0.0136
0.04	2.7248	2.7247	2.6995	0.0487	0.0605	0.0487
0.09	2.5265	2.5201	2.4890	0.1227	0.1497	0.1187
0.16	2.3399	2.3247	2.2917	0.2460	0.2802	0.2278
0.25	2.1678	2.1438	2.1115	0.4091	0.4319	0.3659

[a] $I=1.787$ eV.
[b] $I=3.797$ eV.

model-exchange potential. But in the present context it is also important to note the sensitivity of rotational-excitation cross sections to this potential. In Fig. 1 we compare ANR cross sections $\sigma(0\rightarrow 0)$ and $\sigma(0\rightarrow 2)$ calculated using the Σ_g and Σ_u-tuned TFEGE potential (together with the static potential of Sec. III B and the polarization potential of Sec. III D). The greatest percentage difference in $\sigma(0\rightarrow 2)$ that is introduced by using the Σ_g-tuned rather than the Σ_u-tuned potential occurs at scattering energies around 1 eV. The Σ_u-tuned $0\rightarrow 2$ cross sections proved to be consistently closer to their exact-exchange (with polarization) ANR counterparts, which are indicated by the crosses in Fig. 1(a), than the Σ_g-tuned cross sections. [As expected, the reverse holds for the elastic cross section, which, for completeness, is shown in Fig. 1(b).]

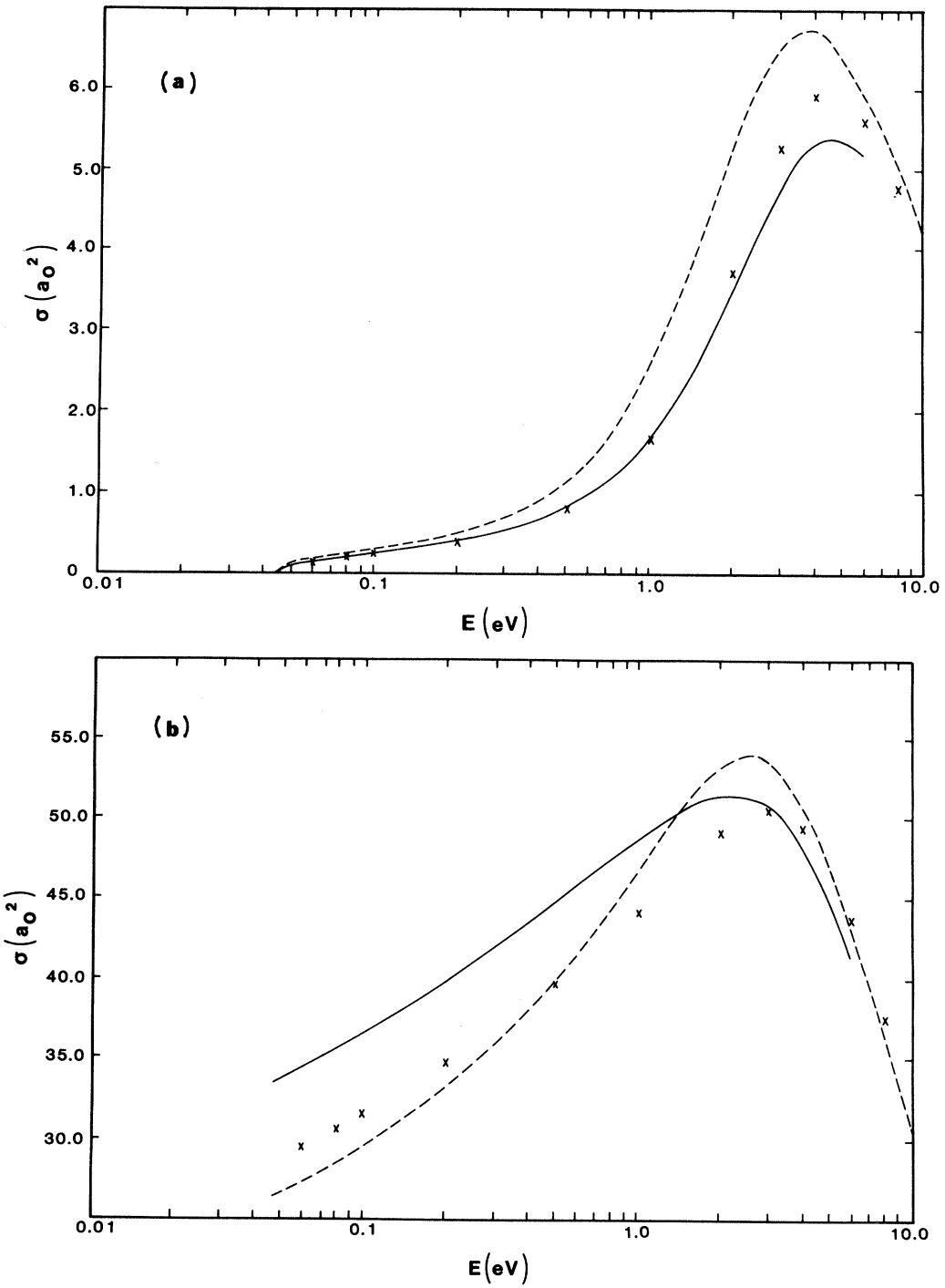

FIG. 1. Integrated e-H_2 cross sections (at $R = 1.4a_0$) for (b) elastic scattering $(0\rightarrow 0)$ and (a) rotational excitation $(0\rightarrow 2)$ using various treatments of exchange. All cross sections were calculated using the ANR theory of Sec. II B. The solid (Σ_u-tuned) and dashed (Σ_g-tuned) curves correspond to TFEGE potentials (see Sec. III C). The crosses come from calculations in which exchange is included exactly (see also Table I).

The R variation of the Σ_u-tuned TFEGE potential will be discussed in a future paper in this series. We consider the determination of $I(R)$ in (34) to be a part of the construction of a representation of the interaction potential for use in the LFCC and AN calculations, noting again that it does not entail adjustment of this potential to experimental data. The use of such a model-exchange potential represents a compromise between demands of accuracy, computational practicality, and extensibility of the present theory to more complex systems. Within these constraints, we believe the present potential to be optimal for inelastic scattering and accept the consequent error in the elastic cross sections.

D. Induced polarization

The final component of the interaction potential models induced-polarization effects. Rigorously, these effects can be incorporated in quantum-mechanical scattering formalisms by allowing for virtual electronic excitations.[42] As with exchange, an exact treatment of polarization leads to prohibitive computational difficulties,[81] so we turn to a model potential, $V_{\rm pot}(\vec{r},R)$ in (32). This term is the decrease in the energy of the electron-molecule system due to the aforementioned distortion. The polarization potential is of especial concern in the present study because its $\lambda=2$ Legendre coefficient $v_2^{\rm pol}(r,R)$ has a long-range r^{-4} dependence that is instrumental in near-threshold rotational excitation.[59(b)]

The model polarization potential that is most widely used in electron-molecule scattering calculations[2-4] is a semiempirical form based on the known asymptotic behavior of $V_{\rm pol}(\vec{r},R)$. This form is predicated on yet another adiabatic approximation: the assumption that the position of the scattering electron $\vec{r}$ can be treated as slowly varying when compared to the response of the target charge density. This approximation fails spectacularly at small r, where short-range correlation effects result in a significant weakening of the polarization potential. In the semiempirical form, these nonadiabatic effects are very crudely mocked by a spherically symmetric cutoff function that contains a parameter (the cutoff radius) that is usually determined by adjusting theoretical cross sections to experimental data. In the present study, this procedure would introduce an undesirable bias in favor of a particular experiment and, owing to the sensitivity of the near-threshold nuclear-excitation cross sections to nonspherical components of the interaction potential, is too crude for our needs.

In our original study of the ANR theory[39] we used an alternative parameter-free analytic polarization potential based on the variation-perturbation calculations of Lane and Henry.[82] This potential, which is available only for the equilibrium H_2 geometry, is based on a different ground-state wave function than is used in this study and had to be scaled by Lane and Henry to ensure the proper asymptotic behavior, a gambit that introduces uncertainty concerning the validity of the potential for small and intermediate values of r.

Recently, Gibson and Morrison[83] developed an *ab initio* e-H_2 polarization potential that does not require scaling. Their $V_{\rm pol}(\vec{r},R)$ is determined from self-consistent-field calculations using the H_2 basis described in Sec. III A augmented with additional basis functions chosen to allow for the polarization distortion. Nonadiabatic effects are incorporated in this potential approximately via a procedure originally introduced by Temkin.[84] The spherical and nonspherical polarizabilities at $R=1.4a_0$ that are determined from the asymptotic form of this polarization potential are $\alpha_0=5.20a_0^3$ and $\alpha_2=1.32a_0^3$. The procedure and codes developed by Gibson and Morrison[83] are easily extensible to nonequilibrium geometries and to other systems and are used throughout this study.

IV. COMPUTATIONAL PROCEDURES

The coupled differential scattering equations—(8) in the LFCC formulation and (18) in the BF-FN theory—are solved numerically using an integral-equations algorithm that has been fully described elsewhere.[85] Briefly, these sets of equations are converted to integral equations, using standard Green's functions procedures, and solved by numerical quadrature to obtain the K matrix at the final mesh point of the radial integration, $r_{\rm max}$. Ideally, the value of $r_{\rm max}$ should be chosen so that all cross sections calculated from the K matrix are converged with respect to this parameter.

For near-threshold inelastic cross sections, this requirement calls for an extremely large value of $r_{\rm max}$; such a value is undesirable because it increases the requisite computer time, and, more seriously, because it increases the cumulative error in the resulting K-matrix elements. A strategy for dealing with this problem is described in Sec. IV A.

Additional difficulties attend the evaluation of differential cross sections for the excitations of interest in the present research. Surmounting these via judicious use of the Born approximation is discussed in Secs. IV B and IV C. Finally, in IV D, we present the parameters used in the scattering calculations reported in Sec. V.

A. Evaluation of K-matrix elements

To allow reasonable choices of $r_{\rm max}$ and still ensure accurate K-matrix elements, we use the FBA to complete the integral over r that formally determines these elements. The need for this tactic and how it is implemented can be seen by examining the integral equation for the K matrix,[62] which we write here in a general form appropriate to either the LFCC or BF-FN formulations,

$$K_{\alpha\beta}(0,\infty)=-2(k_\alpha k_\beta)^{-1/2}\times\sum_\gamma\int_0^\infty \hat{j}_{l_\alpha}(k_\alpha r)V_{\alpha\gamma}(r)u_{\gamma\beta}(r)dr\ , \tag{35}$$

where in the LFCC theory (Sec. II A)

$$\alpha=(v',j',l'),\ \beta=(v'',j'',l''),\ \gamma=(\bar{v}\bar{j}\bar{l})\ ,$$
$$K_{\alpha\beta}=K^J_{v'j'l',v''j''l''}\ , \tag{36a}$$
$$u_{\alpha\beta}=u^J_{v'j'l',v''j''l''}(r)$$

and in the BF-FN theory (Sec. II B)

$$\alpha=l',\ \beta=l'',\ \gamma=\bar{l},\ K_{\alpha\beta}=K^{\Lambda}_{l'l''}(R)\ ,$$
$$k_\alpha=k_\beta=k_b,\ u_{\alpha\beta}=w^{\Lambda}_{ll_0}(r;R)\ . \tag{36b}$$

The arguments on $K_{\alpha\beta}$ in (35) explicitly denote the limits of integration.

The numerical solution of the coupled scattering equations yields $K_{\alpha\beta}(0,r_{\max})$. For a reasonable choice of $r_{\max}$ the residual contribution to (35), $K_{\alpha\beta}(r_{\max},\infty)$, is usually negligible. It arises from distortions of the scattering function by the long-range interaction potential, which, for $r\gtrsim r_{\max}$, is simply

$$V_{\rm int}(\vec{r},R)\simeq V_{\rm pol}(\vec{r},R)$$
$$\sim\frac{\alpha_0(R)}{2r^4}+\left[-\frac{\alpha_2(R)}{2r^4}+\frac{q(R)}{r^3}\right]P_2(\cos\theta)\ ,$$
$$\text{as } r\to\infty\ . \tag{37}$$

However, the long-range region contributes significantly to the distortion of the scattering function for near-threshold excitations, and $K_{\alpha\beta}(r_{\max},\infty)$ cannot be cavalierly neglected. Fortunately, this additional term can be accurately calculated in the FBA, using (37) as the potential energy, and we can approximate (35) by

$$K_{\alpha\beta}(0,\infty)\simeq K_{\alpha\beta}(0,r_{\max})+K^{\rm FBA}_{\alpha\beta}(r_{\max},\infty)\ . \tag{38}$$

The first term in (38) is evaluated by solution of the coupled equations with the full interaction potential (32). The second term is most conveniently calculated by exploiting the simple analytic forms for $K^{\rm FBA}_{\alpha\beta}(0,\infty)$ given in the Appendix. To do so, we use the integral equations code with the potential energy (37) and appropriate modifications to compute the FBA to $K_{\alpha\beta}(0,r_{\max})$. The desired correction term in (38) is then just

$$K^{\rm FBA}_{\alpha\beta}(r_{\max},\infty)=K^{\rm FBA}_{\alpha\beta}(0,\infty)-K^{\rm FBA}_{\alpha\beta}(0,r_{\max})\ . \tag{39}$$

This procedure for completing the radial integral in (35) to infinity is implemented in the present LFCC and BF-FN calculations. To illustrate the importance of the correction term, we show in Table II its effect on the LFCC matrix elements K^J_{jl,j_0l_0} for the $j_0=0\to j=2$ scattering process in the e-H_2 system (with $R=1.4a_0$) at an incident energy of 47 meV. The integrated cross section at this energy is $0.0578a_0^2$ [including contributions through $J=5$ in Eq. (17)]; 86% of this value comes from the term containing $T^2_{20,02}$.

Also shown in Table II is the first Born approximate $K^{\rm FBA}(0,\infty)$; the difference between this matrix element and the coupled-channel counterpart as determined from (38) is indicative of the surprising inadequacy of the FBA for rotational excitation (47 meV is a mere 3 meV above the threshold for the $0\to2$ excitation). We shall return to this matter in Sec. V C.

B. Evaluation of differential cross sections

The formula for the evaluation of the differential cross section $d\sigma/d\Omega(v_0j_0\to vj)$ from the elements of $\underline{T}^J$ in the coupled-angular-momentum LFCC theory[86] entails a two-fold infinite summation over the total-angular-momentum quantum number J (in addition to numerous sums over partial-wave orders). At low scattering energies, where individual terms in this sum can be quite small, a large number of terms are often required to fully converge the cross section. A similar problem arises in AN theory,[4] where the offending summation is over Λ. To deal with these problems, two previously proposed strategies have been combined and adapted to the present calculations; their use leads to a significant reduction of computer time and numerical error. Both strategies are based in part on use of the FBA matrix elements (see Appendix) where appropriate. Their basic idea and implementation in the calculations of Sec. V will be described here; derivations and full equations appear in the original references cited below.

1. *Angular-momentum recoupling*

In order to simplify the evaluation of the differential cross section, Fano and Dill[87] proposed an alternative to the conventional coupled-angular-momentum scheme. Their procedure, as applied to the electron-molecule system at hand, is based on the angular momentum transferred from the orbital motion of the scattered electron to the rotational motion of the target; this "recoupled" angular momentum is $\hat{\vec{l}}_t=\hat{\vec{j}}-\hat{\vec{j}}_0=\hat{\vec{l}}-\hat{\vec{l}}_0$. The cross-section formulas are recast in terms of T matrices defined in a basis in which l_t is a good quantum number. The elements of these matrices can be obtained from those of $\underline{T}^J$ via the transformation

TABLE II. LFCC K-matrix elements for the $j_0=0\to j=2$ excitation in e-H_2 ($R=1.4a_0$) scattering at 47 meV. For this calculation, the coupled equations were integrated to $r_{\max}=130a_0$ ($1.0^{-2}=1.0\times10^{-2}$).

J	Parity[a]	$j_0\ l_0$	$j\ l$	$K(0,r_{\max})$[b]	$K(0,\infty)$[c]	$K^{\rm FBA}(0,\infty)$
0	e	0 0	2 2	0.406^{-4}	0.515^{-4}	0.569^{-4}
1	o	0 1	2 1	-0.658^{-3}	-0.711^{-3}	-0.662^{-3}
2	e	0 2	2 0	0.166^{-2}	0.165^{-2}	0.175^{-2}
2	e	0 2	2 2	-0.523^{-4}	-0.542^{-4}	-0.540^{-4}
2	e	0 2	2 4	-0.443^{-6}	0.304^{-6}	0.304^{-6}

[a]Parity is even (odd) according to whether $j+l=j_0+l_0$ is even (odd).
[b]From converged close-coupling calculations (see Sec. IV D).
[c]From Eq. (38).

$$T^{l_t}_{vjl,v_0j_0l_0}=\sum_J(-1)^J(2J+1)\begin{Bmatrix} j_0 & j & l_t \\ l & l_0 & J \end{Bmatrix}T^J_{vjl,v_0j_0l_0}\ , \tag{40}$$

where $\{\cdots\}$ is a 6-j symbol and the sum over J is constrained by the triangle rules $\Delta(j_0,l_0,J)$ and $\Delta(j,l,J)$. The resulting equations for $d\sigma/d\Omega(v_0,j_0\to v,j)$ have been derived and discussed by Chandra.[31]

A similar transformation can be performed on the AN matrix elements $\langle\phi_v\,|\,T^\Lambda_{ll_0}(R)\,|\,\phi_{v_0}\rangle$ [or, in the ANR theory, on $T^\Lambda_{ll_0}(R_{\rm eq})$], changing the body representation to one in which l_t rather than Λ is a good quantum number, viz.,

$$T^{l_t}_{vl,v_0l_0}=\sum_\Lambda(-1)^\Lambda C(l,l_0,l_t;\Lambda,-\Lambda,0)\times\langle\phi_v\,|\,T^\Lambda_{ll_0}(R)\,|\,\phi_{v_0}\rangle\ , \tag{41}$$

where the sum over Λ runs from $|l-l_0|$ to $l+l_0$. Introduction of l_t into the AN theory enables one to define differential cross sections (that are partial in l_t) in which the rotational dynamics do not appear. The advantages of doing so, as well as full equations for the resulting cross sections, have been discussed by Norcross and Padial.[26]

In addition to considerably simplifying the structure of the equation that must be used to evaluate $d\sigma/d\Omega(v_0,j_0\to v,j)$, the angular-momentum-recoupling scheme is operationally very convenient when combined with the FBA in the closure formulas of Sec. IV B 3. We use this representation in our LFCC, ANR, and EMA studies.

2. *Use of the first Born approximation*

The evaluation of differential cross sections in any of the formulations considered in this research inevitably requires T-matrix elements for large partial-wave orders (l and l_0). Because of the presence of strong repulsive centrifugal-potential terms in the corresponding coupled scattering equations, these matrix elements can be accurately determined in the FBA using the long-range part of the potential energy [Eq. (37)]. Analytic expressions for these matrix elements in the LFCC and BF-FN theories are given in the Appendix.[88]

Following Norcross and Padial,[26] we introduce a "Born order" l_B such that T-matrix elements for $l\geq l_B$ and $l_0\geq l_B$ are given (to the desired accuracy) by their FBA counterparts. For e-H_2 collisions in the energy range studied, $l_B=3$ is adequate to obtain better than 1% accuracy.

The FBA matrix elements of the Appendix are used (1) to calculate the LFCC l_t-reduced T-matrix elements (40) for all required values of J if $l_0\geq l_B$ and $l\geq l_B$, and (2) to calculate the AN matrix elements (41) for all Λ if $l_0\geq l_B$ and $l\geq l_B$. All other T-matrix elements that must be used to calculate converged differential cross sections are determined via close-coupling calculations using the full interaction potential.

3. *Closure formulas*

The fact that large-order T-matrix elements can be accurately approximated using the FBA was exploited by Crawford and Dalgarno[35] to develop an alternative formula for differential cross sections for electron–polar-molecule scattering in the LFCC coupled-angular-momentum formulation. Their derivation is also based on triangle relations derived from algebraic coefficients that appear in the equation for $d\sigma/d\Omega(v_0j_0\to vj)$; the resulting expression requires only a finite number of T-matrix elements, many of which can be evaluated in the FBA.

This strategy forms the basis of the multipole-extracted adiabatic-nuclei (MEAN) theory of Norcross and Padial.[26] This approximation, which was originally proposed for electron–polar-molecule systems, entails the use of coupled-channel BF-FN T-matrix elements for low partial-wave orders and LFCC-FBA matrix elements for large orders.

In the present implementation, we use the closure formulas of Crawford and Dalgarno[36] in the l_t-reduced formulation of Sec. IV B 1 to obtain the LFCC differential cross section via

$$\frac{d\sigma}{d\Omega}(v_0,j_0\to v,j)=\frac{d\sigma_B}{d\Omega}(v_0,j_0\to v,j)+\frac{1}{4k_0^2}\sum_{\lambda=0}^{\lambda_{\max}}[A_\lambda^{(l_B)}(v_0,j_0\to v,j)-A_\lambda^{(0)}(v_0,j_0\to v,j)]\ , \tag{42}$$

where the first term is the analytic expression for this cross section in the FBA. In the second term, the coefficients $A_\lambda^{(l_B)}(v_0j_0\to vj)$, which are given explicitly by Eq. (14) of Ref. 31, contain the reduced T-matrix elements of Eq. (40). All such elements with partial-wave order $\geq l_B$ are evaluated in the FBA of Sec. IV B 3; all other such elements are obtained via Eq. (40) from LFCC calculations. The sum over λ is rapidly convergent; for e-H_2 scattering requisite values of $\lambda_{\max}$ ranged from 10 to 23. Only a limited number of T-matrix elements are needed to evaluate $d\sigma/d\Omega(v_0,j_0\to v,j)$ via Eq. (42); the maximum partial-wave order that contributes to this cross section is $l_B+\lambda_{\max}$.

A similar result obtains from application of the closure formulas to the AN expression for the differential cross sections. Our implementation differs from the MEAN theory[26] in that *all* contributions to $d\sigma/d\Omega(v_0,j_0\to v,j)$, including the analytic FBA term, are calculated within the AN theory. This theoretical consistency is possible only for electron scattering from nonpolar molecules, which is not plagued by the divergent BF-FN cross sections that beset the AN theory for collisions with polar targets. In the ANR calculations reported in Sec. V, $\lambda_{\max}=15$ was used at all energies.

C. Parameters for close-coupling calculations

In order to ensure that the differences between LFCC and approximate (AN or EMA) cross sections are actually indicative of a breakdown in the approximate scattering theory (rather than due to numerical vagaries of the two calculations), we imposed identical (and rather stringent) convergence criteria on both studies. The standard for the results of Sec. V was set by the differential cross sections $d\sigma/d\Omega(j_0 \rightarrow j)$, which are *globally converged*[85] to better than 1% in all parameters of the scattering calculations.

In the LFCC study, this criterion required including all channels $(j,l;J)$ that result from retaining five rotor states and all total angular momenta through $J=5$. The close-coupling equations were integrated to $r_{\max}=130.0a_0$ and the completion formula (38) used to obtain the elements of $\underline{K}^J$. The rotational constant used, $2.7\times10^{-4}E_h$, gives thresholds of 44 and 73 meV for the $0\rightarrow2$ and $1\rightarrow3$ excitations, respectively.

The AN and EMA results are based on BF-FN coupled-channel calculations for five electron-molecule symmetries, corresponding to $\Lambda=0$, 1, and 2. The designations of these symmetries and the number of partial waves (channels) per symmetry are $\Sigma_g(6)$, $\Sigma_u(6)$, $\Pi_u(6)$, $\Pi_g(5)$, and $\Delta_g(5)$. In each symmetry, coupled equations were integrated out to $r_{\max}=170.0a_0$ and Eq. (38) used to complete the calculation of $\underline{K}^\Lambda(R)$.

V. RESULTS AND DISCUSSION

In this section we present and discuss differential and integrated cross sections for the $j_0\rightarrow j$ rotational excitation of H_2 calculated in the three formulations described in Sec. II: the exact LFCC treatment and the ANR and EMA approximations. All cross sections were calculated in the *rigid-rotator approximation* with $R=1.4a_0$ using the interaction potential described in Sec. III. Hence these results do not allow for the vibrational motion of the nuclei and are inappropriate for comparison to experimental cross sections.

The integrated $0\rightarrow2$ and $1\rightarrow3$ cross sections are presented in Tables III and IV and the differential cross sections in Figs. 3 and 4. The qualitative *and quantitative* trends and conclusions discussed below were found to hold for all excitations studied ($0\rightarrow2$, $1\rightarrow3$, $2\rightarrow4$, and $3\rightarrow5$). For the sake of brevity, we shall here focus on the $0\rightarrow2$ excitation.

A. Tests of ANR theory

In the prior literature of the AN theory, a variety of tests of its validity have been proposed.[7,14] In this section, we examine the results of the present calculations from several perspectives, seeking to explore the usefulness of various validity tests as well as the reliability of the ANR theory itself.

1. Total integrated cross sections

The total integrated cross section, which, in the rigid-rotator approximation, is defined as the sum over all energetically accessible final-rotational-state quantum numbers of $\sigma(j_0\rightarrow j)$, can be calculated in the FN approximation[4] directly from the BF T-matrix, $\underline{T}^\Lambda(R)$. As pointed out by Chang and Temkin,[11] the resulting quantity is equal to the sum of the ANR rotational-excitation cross sections $\sigma(j_0\rightarrow j)$ (provided they are not multiplied by the wave-number ratio k_j/k_0 and are calculated with $k_b=k_0$) and should be independent of j_0.

TABLE III. e-H_2 $0\rightarrow2$ integrated rotational-excitation cross sections in a_0^2 from fixed R $(=1.4a_0)$ LFCC (see Sec. II A), ANR (Sec. II B), and EMA (Sec. II D) calculations. The percentage differences of approximate (ANR, EMA) results from LFCC cross sections are shown in Fig. 2. The threshold for this excitation is 0.044 eV.

E (eV)	LFCC	ANR	EMA
0.047	0.058	0.074	0.063
0.050	0.082	0.102	0.089
0.065	0.150	0.178	0.160
0.080	0.192	0.221	0.202
0.10	0.234	0.262	0.242
0.20	0.378	0.408	0.384
0.50	0.784	0.821	0.787
1.0	1.619	1.667	1.622
1.5	2.557	2.609	2.559
2.0	3.450	3.498	3.450
3.0	4.742	4.774	4.740
4.5	5.391	5.399	5.387
6.0	5.201	5.199	5.197

Therefore, at scattering energies where the ANR theory is valid, one would expect to see this j_0 independence in total cross sections obtained from LFCC calculations or, for that matter, from experiment. Moreover, these "accurate" total cross sections should agree with those obtained from ANR calculations if the two studies are internally consistent. The results in Table V show that both of these conditions are well satisfied by the present results, even very near threshold. [These total integrated cross sections include only the elastic and $|\Delta j|=2$ contributions, all other $\sigma(j_0\rightarrow j)$ being negligibly small.]

The agreement between the various cross sections in Table V is not, however, indicative of the reliability of the ANR theory at these energies; rather, it is a consequence of the fact that the elastic cross section $\sigma(j_0\rightarrow j_0)$ is the dominant contribution to the total cross section over the

TABLE IV. e-H_2 $1\rightarrow3$ integrated rotational-excitation cross sections in a_0^2; see caption to Table III. The threshold for this excitation is 0.073 eV.

E (eV)	LFCC	ANR	EMA
0.080	0.040	0.057	0.048
0.100	0.083	0.108	0.092
0.200	0.191	0.220	0.198
0.500	0.439	0.476	0.443
1.000	0.937	0.985	0.940
1.500	1.498	1.550	1.500
2.000	2.034	2.083	2.035
3.000	2.817	2.850	2.817
4.500	3.219	3.229	3.217
6.000	3.113	3.112	3.111

TABLE V. Total integrated cross sections (in a_0^2) and elastic cross sections (in parentheses) for e-H_2 scattering at $R=1.4a_0$. LFCC results include $j_0\rightarrow j_0$ and $j_0\rightarrow j_0+2$. ANR theory predicts that these cross sections will be independent of the initial-state quantum number j_0. Also shown are results from a separate ANR calculation (including the factors k_j/k_0).

	LFCC			
E (eV)	$j_0=0$	$j_0=1$	$j_0=2$[a]	ANR
0.047	33.63	33.73	33.77	33.62
	(33.57)	(33.73)	(33.69)	(33.55)[b]
0.080	35.83	35.86	35.85	35.84
	(35.64)	(35.82)	(35.76)	(35.61)
0.100	36.83	36.89	36.83	36.84
	(36.60)	(36.79)	(36.74)	(36.58)
0.200	40.29	40.34	40.32	40.31
	(39.91)	(40.15)	(40.08)	(39.90)
0.500	45.65	45.70	45.68	45.68
	(44.87)	(45.26)	(45.15)	(44.86)
1.000	50.36	50.36	50.39	50.40
	(48.74)	(49.42)	(49.26)	(48.74)
4.500	52.21	52.22	52.21	52.18
	(46.82)	(49.01)	(48.37)	(46.78)

[a]Includes superelastic contribution $2\rightarrow 0$.
[b]For $j_0=0$.

whole energy range studied. As can be seen by examining the elastic contributions, which are shown in parentheses in Table V, they are orders of magnitude larger than $\sigma(0\rightarrow 2)$ (Table III), and the ANR theory is quite successful at predicting $\sigma(j_0\rightarrow j_0)$. To draw conclusions about the validity of ANR theory a more sensitive test is needed.

2. *Ratio test*

The ANR theory predicts that cross sections for two different rotational excitations $j_0\rightarrow j$ and $j_0'\rightarrow j'$ will obey the simple relationship

$$\frac{\sigma(j_0'\rightarrow j')}{\sigma(j_0\rightarrow j)}=\frac{k_{j'}}{k_j}\left[\frac{C(j_0',2,j';0,0,0)}{C(j_0,2,j;0,0,0)}\right]^2, \tag{43}$$

where $k_{j'}$ and k_j are the final-state wave numbers of the scattering electron for the two excitations [cf. Eq. (4)]. The cross sections in (43) are evaluated at the same body-frame energy E_b. This relationship has been extensively described by Chang and Temkin,[11] by Shimamura,[22,25] and by Norcross;[24] the latter authors use it to develop very useful expressions for stopping cross sections. At energies where this relationship holds, it can trivially be used to predict a plethora of rotational-excitation cross sections $\sigma(j_0'\rightarrow j')$ from *a single* set of accurate (LFCC or experimental) results $\sigma(j_0\rightarrow j)$; such a strategy is of enormous value in, for example, transport analysis of swarm experiments, where numerous excitations must be taken into account.[40]

The validity of Eq. (43) for the $0\rightarrow 2$ and $1\rightarrow 3$ cross sections is examined in Table VI, where a deterioration in the ANR predictions can be seen as the scattering energy is decreased to 0.073 eV, the threshold for the $1\rightarrow 3$ excitation. At energies below $\sim$0.5 eV, the EMA described in Sec. II D consistently yields ratios that are in better agreement with the accurate LFCC ratios than those predicted by Eq. (43).

TABLE VI. Ratio $\sigma(1\rightarrow 3)/\sigma(0\rightarrow 2)$ for e-H_2 scattering ($R=1.4a_0$).

	ANR theory	Calculations		
E (eV)	[Eq. (43)]	LFCC	ANR	EMA
0.080	0.265	0.208	0.258	0.238
0.100	0.417	0.355	0.412	0.380
0.200	0.541	0.505	0.539	0.516
0.500	0.581	0.560	0.580	0.563
1.000	0.591	0.579	0.591	0.579
4.500	0.598	0.597	0.598	0.597

This comparison suggests that the ANR theory could reliably be used for e-H_2 scattering at energies above $\sim$0.5 eV (many times the meV thresholds characteristic of this system). However, caution clearly should be exercised in using Eq. (43) to predict near-threshold rotational-excitation cross sections. It is interesting to note that this equation fails near threshold not because of a breakdown in the linear dependence of $\sigma(1\rightarrow 3)/\sigma(0\rightarrow 2)$ on k_3/k_2, but rather because the proportionality constant is different from the simple factor in Eq. (43).

3. *Direct comparison*

Obviously, the most precise test of the ANR theory is a direct comparison of ANR rotational-excitation cross sections with those produced in LFCC calculations. Such comparisons are presented for the $0\rightarrow 2$ and $1\rightarrow 3$ excitations in Tables III and IV. The ANR cross sections are seen to be larger than their LFCC counterparts. The percentage difference between the two for the $0\rightarrow 2$ excitation is given by the solid curve in Fig. 2. At the lowest energy considered, 0.047 eV (3 meV above threshold), the ANR cross section is too large by 28%. The corresponding ANR differential cross section, which is compared to the LFCC result in Fig. 3(a), does not exhibit even qualitatively correct dependence on scattering angle.

With increasing energy, the ANR cross sections improve as expected, although at 0.5 eV (roughly 11 times threshold), they are still in error by 5%. The differential cross sections of Fig. 3 ($0\rightarrow 2$) and Fig. 4 ($1\rightarrow 3$) reveal more serious deficiencies in the predictions of ANR theory. Note especially the pronounced dip in the forward direction exhibited by the LFCC differential cross sections at energies near 0.1 eV. This structure is not reproduced by the ANR theory (because of the incorrect behavior of the ANR $l=l_0=1$ T-matrix elements in this energy range). The integrated cross sections do not accurately reflect the severity of the disagreement between the ANR and LFCC theories at these energies because they deemphasize forward-angle scattering.

As the scattering energy is further increased above 1 eV (roughly 23 times threshold), the ANR differential cross sections come into excellent agreement with their LFCC counterparts. This improvement is, of course, reflected in the integrated cross sections of Tables III and IV. Although the AN theory is expected to break down for

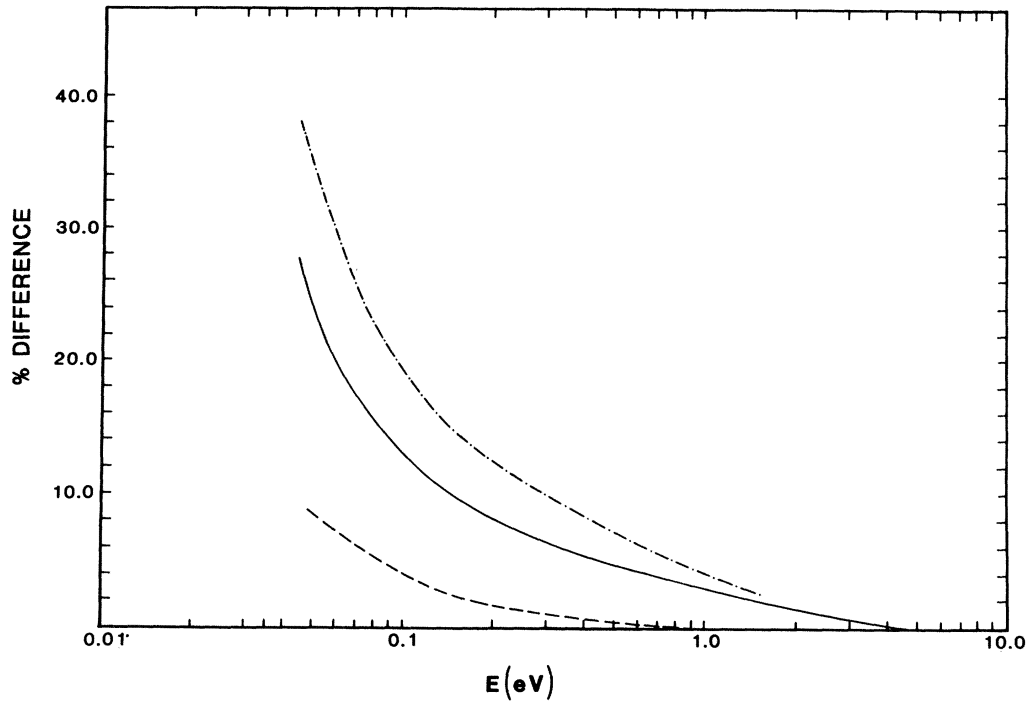

FIG. 2. Percentage deviation of approximate e-H_2 integrated cross sections for the $0\rightarrow 2$ excitation from their LFCC counterparts (see Tables III and IV). Solid and dashed curves correspond to the ANR (Sec. II B) and EMA (Sec. II D) formalisms, respectively, using the Σ_u-tuned FEG exchange potential described in Sec. III C. Dotted-dashed curve corresponds to the ANR theory using the Σ_g-tuned FEG exchange potential.

scattering near a resonance energy, no deterioration in the ANR cross sections is seen near the 3-eV "enhancement" of $\sigma(j_0\rightarrow j)$; presumably this is a consequence of the breadth of this "resonance."

In the discussion of AN theory in Sec. II B and of the interaction potential in Sec. III, we emphasized the theoretical importance of using an accurate potential in any investigation of the validity of the AN formulation. The sensitivity of such a study to V_{int} is strikingly demonstrated by comparing the solid curve in Fig. 2, which gives the percent error in the ANR $\sigma(0\rightarrow 2)$, with the dotted-dashed curve in this figure, which shows the same quantity calculated from ANR and LFCC cross sections determined in our preliminary study.[39] (The differences between the potential energies used to generate these curves are discussed in Sec. III.) It is important in this context to note that the potential energy used in Ref. 39 (dotted-dashed curve in Fig. 2) is reasonably accurate; indeed, it produces total and rotational excitation cross sections that are in good agreement with experimental results.[89]

This comparison, in turn, calls into question the accuracy of the present interaction potential. A meaningful comparison of theoretical and experimental cross sections (at the level of numerical accuracy of the present calculations) should allow for vibrational motion in the former results. Such a comparison is forthcoming; the calculated LFCC rovibrational $j_0=0\rightarrow j=2$ cross sections (within the ground vibrational state) are found to agree with the highly accurate swarm results of Crompton *et al.*[90] to within the experimental error bars. This agreement strongly suggests that the potential energy used in the present study is a very good approximation to the true e-H_2 interaction (for rotational excitation).

B. The EMA

The EMA integrated cross sections are given in Tables III and IV, and their percentage error is shown by the dashed curve in Fig. 2. These results show a striking improvement over the ANR cross sections near threshold; for example, at a scattering energy of 0.065 eV, the EMA yields a $0\rightarrow 2$ cross section that differs from the LFCC $\sigma(0\rightarrow 2)$ by only 7%, as compared to a 19% error in the ANR result. For energies above 1 eV, the EMA integrated $j_0\rightarrow j$ cross sections are within 1% of their LFCC counterparts.

The EMA of Sec. II D is less successful at reproducing the LFCC differential cross sections for rotational excitation, as illustrated in Figs. 3 and 4. Only at energies above about 1 eV does the EMA properly predict the angle dependence of the LFCC results. Evidently, a more sophisticated modification of the ANR theory is required to enable one to determine accurate $d\sigma/d\Omega(j_0\rightarrow j)$ without resorting to a full LFCC calculation.

C. The first Born approximation

The use of the FBA to calculate near-threshold $\Delta j=2$ cross sections for electron-molecule collisions is theoretically grounded in the weak nature of the long-range potential (37) that determines these cross sections. Since the FBA is obtained by retaining only the first term in the Born series,[45] and since all higher-order terms in this series vanish at threshold, the FBA should, indeed, be

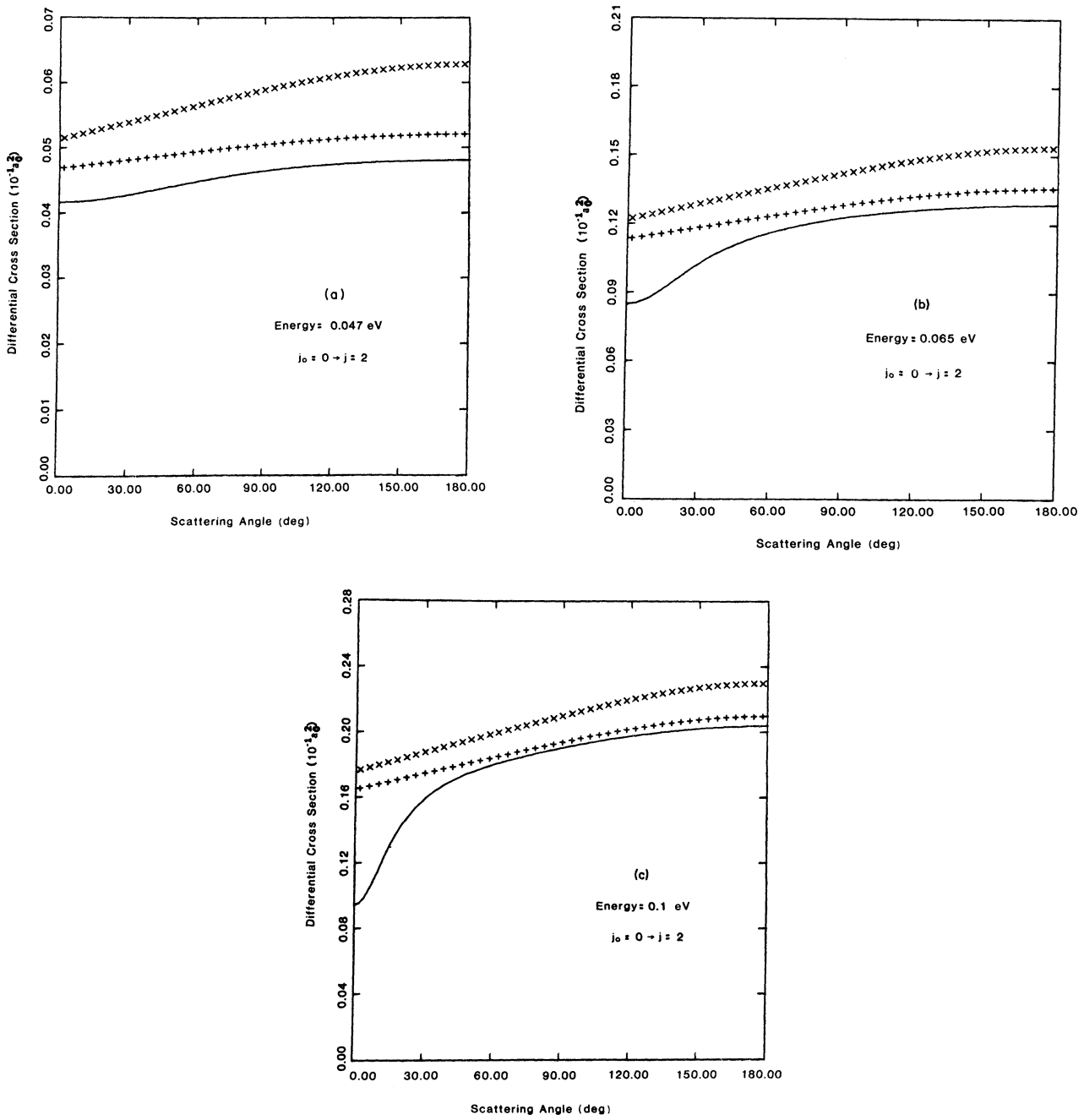

FIG. 3. Differential cross sections for the $0 \rightarrow 2$ rotational excitation of H_2 in the LFCC (solid curve), ANR ($\times$), and EMA ($+$) formalisms of Sec. II. All results are for $R = 1.4a_0$. Scattering energies are (a) 47 meV, (b) 65 meV, (c) 0.1 eV, (d) 1.5 eV, and (e) 6.0 eV.

valid at energies near enough to the excitation threshold. The question is "how near is 'near enough'"?

In Table II, laboratory-frame FBA K-matrix elements at 47 meV that are important for the $0 \rightarrow 2$ cross sections were shown to disagree with the corresponding LFCC matrix elements. In Table VII, such a comparison is shown (for the two most important elements) at energies from 0.2 meV above threshold to 500 meV. Even at the lowest of these energies, the laboratory-frame FBA K-matrix elements are in error by several percent.

An indication of the impact of this disagreement on the integrated $0 \rightarrow 2$ cross sections is provided by the results shown in Table VIII. As pointed out in Sec. II C, the AN FBA matrix elements that are obtained by frame-transforming the BF-FN FBA T matrix are formally different from the corresponding LFCC T-matrix elements. This facet of the FBA is also illustrated in Table VIII. In either the ANR or LFCC formulations, a non-negligible disparity is evident between the close-coupling and FBA cross sections.

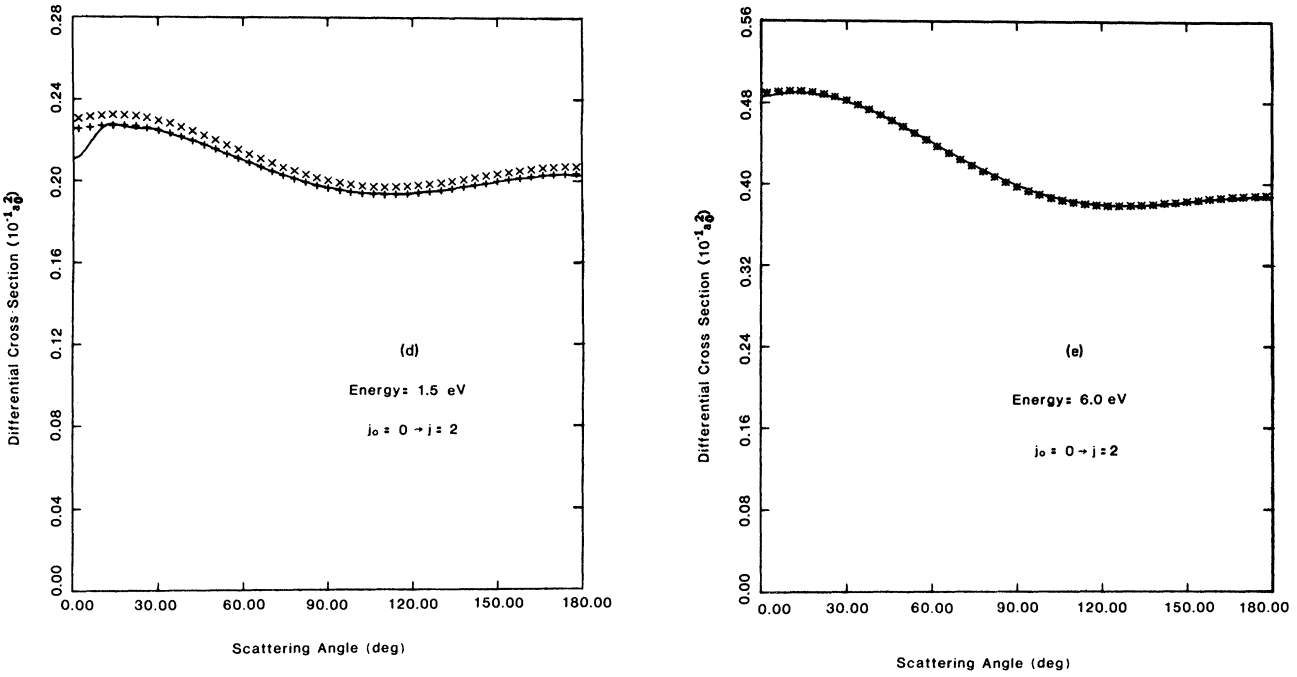

FIG. 3. (*Continued.*)

VI. CONCLUSIONS

In the present study we have quantified the expected breakdown of the ANR theory near threshold for e-H_2 scattering and explored one alternative, an implementation of Nesbet's EMA. The central results of this study can be found in the percentage-difference curves of Fig. 2 and the differential-cross-section comparisons of Figs. 3 and 4.

We have found that conventional ANR theory yields reasonably accurate integrated cross sections for body energies above about 0.5 eV and qualitatively correct differential cross sections above a few eV. Theoretical results derived from this theory, in particular, the handy ratio relationship (43) between integrated cross sections for different excitations, are reliable above about 1 eV. These findings paint a somewhat less encouraging picture of the usefulness of ANR theory than do the rough qualitative estimates of its region of validity that have been published heretofore.

The reason for the failure of this formulation lies in its incorrent prediction of the threshold behavior of certain T-matrix elements on which the excitation cross sections critically depend (cf. Sec. II C). This defect is repaired by our implementation of the EMA to the extent that this theory yields much more accurate *integrated* cross sections than does the ANR formalism. To attain comparable accuracy in *differential* excitation cross sections evidently requires a more sophisticated strategy for coping with the threshold behavior of the T matrix.

Finally, we note the surprisingly strong dependence of the validity of adiabatic theories such as the ANR and (to a lesser extent) the EMA on the representation of the interaction potential, as illustrated in Fig. 2. This observation emphasizes the need for accurate models of this potential for electron-molecule scattering and reveals a fascinating interdependence between the approximations chosen to render the scattering theory tractable and those used to obtain practical potential energies.

Apart from the limitations on the interaction potential discussed in Sec. III, the principal restriction of the

TABLE VII. LFCC K-matrix elements for $j'=2$, $j''=0$ for e-H_2 scattering compared to corresponding elements as determined in the FBA using the potential energy of Eq. (37) ($1.0^{-2}=1.0\times10^{-2}$).

	$l'=1$, $l''=1$ ($J=1$)		$l'=0$, $l''=2$ ($J=2$)	
E (meV)	LFCC	FBA	LFCC	FBA
44.2	-0.722^{-4}	-0.675^{-4}	0.798^{-3}	0.846^{-3}
45.0	-0.309^{-3}	-0.288^{-3}	0.128^{-2}	0.136^{-2}
47.0	-0.711^{-3}	-0.662^{-3}	0.165^{-2}	0.175^{-2}
50.0	-0.118^{-2}	-0.109^{-2}	0.189^{-2}	0.200^{-2}
65.0	-0.281^{-2}	-0.253^{-2}	0.222^{-2}	0.235^{-2}
80.0	-0.399^{-2}	-0.353^{-2}	0.230^{-2}	0.243^{-2}
100.0	-0.532^{-2}	-0.456^{-2}	0.236^{-2}	0.250^{-2}
200.0	-0.107^{-1}	-0.803^{-2}	0.268^{-2}	0.291^{-2}
500.0	-0.262^{-1}	-0.146^{-1}	0.366^{-2}	0.430^{-2}

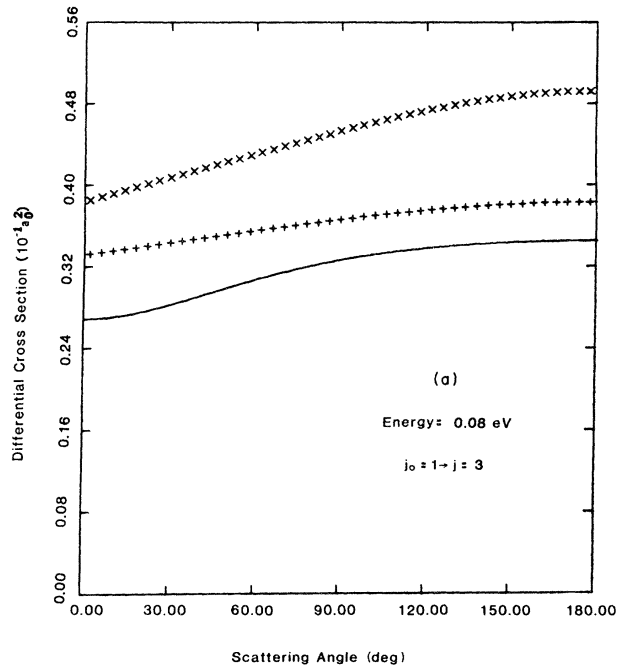

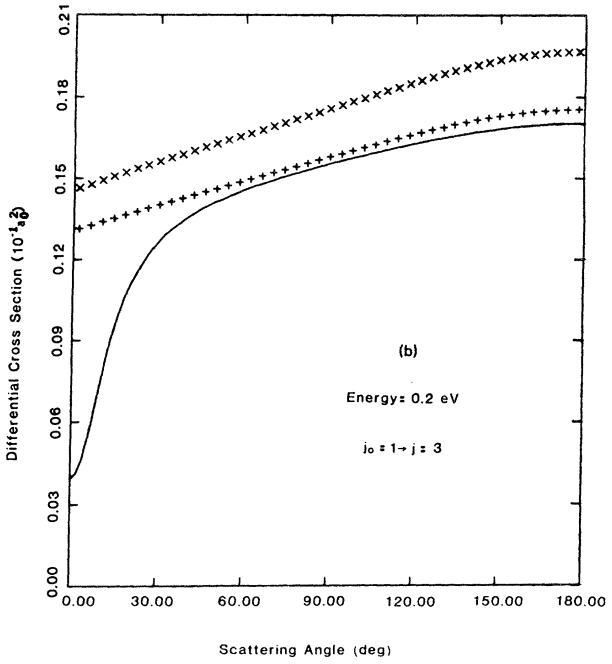

FIG. 4. Same as Fig. 3 for the $1 \rightarrow 3$ excitation at scattering energies of (a) 80 meV and (b) 0.2 eV.

present work is the rigid-rotor approximation. Inclusion of the vibrational Hamiltonian in LFCC and AN calculations[92] increases the integrated cross sections from both studies, bringing the former into close agreement with experimental results, and markedly alters the shape of the differential cross sections. Moreover, the conclusions of this paper cannot be generalized to answer the question of usefulness of an adiabatic treatment of the vibrational motion; this matter must be addressed by analogous comparisons using the full theories of Secs. II A and II B.

TABLE VIII. Test of the FBA for near-threshold e-H_2 scattering. Cross sections $\sigma(0 \rightarrow 2)$ in a_0^2 from FBA calculations (see Appendix) using the potential energy of Eq. (37) are compared to results from coupled-channel (CC) calculations in the LFCC ANR formulations. The threshold for this excitation is 0.044 eV. For scattering energies above 0.1 eV, the FBA cross sections deviate substantially from their CC counterparts.

	Laboratory frame		Body frame (ANR)	
E (eV)	CC	FBA	CC	FBA
0.047	0.058	0.063	0.074	0.065
0.050	0.082	0.088	0.103	0.090
0.065	0.150	0.147	0.178	0.151
0.080	0.192	0.177	0.221	0.181
0.100	0.202	0.234	0.262	0.206

Such comparisons for the e-H_2 systems, investigations of new nonadiabatic theories for near-threshold excitations, and extensions of the present research to more complicated systems will be the immediate topics of future papers in this series.

ACKNOWLEDGMENTS

The authors are deeply grateful to Dr. Tom Gibson for his assistance with many phases of this project, to Dr. Nely Padial for sending us a program for evaluation of ANR differential cross sections, and to Dr. D. W. Norcross, Dr. N. F. Lane, Dr. L. A. Collins, and Dr. G. A. Parker for their insights and comments on various aspects of this research. This work was supported by the Office of Basic Energy Sciences, U.S. Department of Energy. One of us (M.A.M.) acknowledges additional support by a grant from The Research Corporation.

APPENDIX

In this appendix, we draw together and outline the derivation of FBA expressions for T-matrix elements in the LFCC and AN theories;[88] the latter are based on the implementation of the FBA for the BF-FN T matrix.

The reactance matrix $\underline{K}$ [in either the LFCC formulation, $\underline{K}^J$, or in the FN formulation, $\underline{K}^\Lambda(R)$] is related to the matrix of radial scattering functions that solve the coupled scattering equations by the integral equation (35). The FBA to this matrix is obtained by simply replacing $u_{\alpha\beta}(r)$ [see Eq. (36) for notation] by the spherical free wave function (the Ricatti Bessel function)[45] $\hat{j}_l(k_\alpha r)\delta_{\alpha\gamma}$. In this Appendix, we shall work with the T matrix, which, in the FBA, has matrix elements

$$T_{\alpha\beta} = -2iK_{\alpha\beta} \tag{A1}$$

$$= \frac{4i}{\sqrt{k_\alpha k_\beta}} \int_0^\infty \hat{j}_l(k_\alpha r) V_{\alpha\beta}(r) \hat{j}_{l_0}(k_\beta r) dr \ . \tag{A2}$$

In the LFCC formulation (Sec. II A), the integral (A2) can be simplified using the angular-coupling coefficients, viz.,

$$T^J_{vjl,v_0j_0l_0}=4i(k_{vj}k_0)^{1/2}\times\sum_\lambda f_\lambda(j,l;j_0,l_0;J)R^L_\lambda(v,j,l;v_0,j_0,l_0;k_{vj},k_0)\ , \tag{A3}$$

where we have introduced the (laboratory-frame) radial integral

$$R^L_\lambda(v,j,l;v_0,j_0,l_0;k_{vj},k_0)=\int_0^\infty j_l(k_{vj}r)\langle\phi_v(R)\,|\,v_\lambda(r,R)\,|\,\phi_{v_0}(R)\rangle j_{l_0}(k_0r)r^2dr\ . \tag{A4}$$

For a long-range multipole potential term that falls to zero as r^{-s_λ} as $r\to\infty$, the vibrational matrix element in (A4) can be written

$$\langle\phi_v(R)\,|\,v_\lambda(r,R)\,|\,\phi_{v_0}(R)\rangle=B_\lambda(v,v_0)r^{-s_\lambda}\ , \tag{A5}$$

where $B_\lambda(v,v_0)$ is a constant. Then, provided $l+l_0-s_\lambda+3>0$, the radial integral (A4) can be evaluated in terms of gamma functions and confluent hypergeometric functions,[91] the latter approaching unity as $k_{vj}/k_0\to0$, viz.,

$$R^L_\lambda(v,j,l;v_0,j_0,l_0;k_{vj},k_0)=B_\lambda(v,v_0)\pi2^{-s_\lambda}k_{vj}^l k_0^{\,l-s_\lambda+3}\frac{\Gamma\left[\frac{l+l_0-s_\lambda+3}{2}\right]}{\Gamma\left[\frac{l-l_0+s_\lambda}{2}\right]\Gamma(l+\frac{3}{2})}$$

$$\times F\left[\frac{l_0+l-s_\lambda+3}{2},\frac{l-l_0-s_\lambda+2}{2},l+\frac{3}{2};\left[\frac{k_{vj}}{k_0}\right]^2\right]. \tag{A6}$$

The FBA to the laboratory-frame scattering amplitude is obtained from the T matrix of Eq. (A3) via the relation

$$f_{vv_0}(\hat r')=\left[\frac{\pi}{k_{vj}k_0}\right]^{1/2}\sum_\mu i^{l_0-l+1}(-1)^{j_0+j-l_0-l}(2J+1)\sqrt{2l_0+1}\,T^J_{vjk,v_0j_0l_0}Y_{lm_l}(\hat r')$$

$$\times\begin{bmatrix}j_0 & l_0 & J\\ m_{j_0} & 0 & -M\end{bmatrix}\begin{bmatrix}j & l & J\\ m_j & m_l & -M\end{bmatrix}, \tag{A7}$$

where we have chosen $\hat k'_0=\hat z'$, as is conventional in the laboratory-frame formulation. The summation index is $\mu=(J,M,l,l_0,m_l)$. Inserting (A3) into (A7), carrying out the summations over J and M, and using the triangle rule on (l,l_0,λ), we obtain

$$f_{vv_0}(\hat r')=-4[\pi(2j_0+1)(2j+1)]^{1/2}$$

$$\times\sum_{l,l_0,m_l}\sum_\lambda i^{l_0-l}(-1)^{m_{j_0}-m_l}[(2l_0+1)(2l+1)]^{1/2}Y_{lm_l}(\hat r')$$

$$\times\begin{bmatrix}j_0 & j & \lambda\\ 0 & 0 & 0\end{bmatrix}\begin{bmatrix}l_0 & l & \lambda\\ 0 & 0 & 0\end{bmatrix}\begin{bmatrix}j_0 & j & \lambda\\ m_{j_0} & -m_j & -m_l\end{bmatrix}\begin{bmatrix}l_0 & l & \lambda\\ 0 & -m_l & m_l\end{bmatrix}R^L_\lambda(v,j,l;v_0,j_0,l_0;k_{vj},k_0)\ . \tag{A8}$$

This expression can be shown to be equivalent to that of Dalgarno and Moffett.[59(b)] The resulting FBA-LFCC differential cross section for the excitation $(v_0,j_0\to v,j)$ can be conveniently written in terms of the radial integral (A4) as

$$\frac{d\sigma}{d\Omega}(v_0,j_0\to v,j)=4\frac{k_{vj}}{k_0}\sum_\eta C_\eta R^L_\lambda(v,j,l'_1;v_0,j_0,l_1;k_{vj},k_0)R^L_\lambda(v,j,l'_2;v_0,j_0,l_2;k_{vj},k_0)P_L(\cos\theta')\ , \tag{A9}$$

where the summation index of $\eta=(l_1,l'_1,l_2,l'_2,\lambda,L)$ and the coefficient C_η is

$$C_\eta\equiv\left[\frac{2j+1}{2\lambda+1}\right]^{1/2}\begin{bmatrix}j_0 & j & \lambda\\ 0 & 0 & 0\end{bmatrix}^2 i^{l_2-l_1+l'_1-l'_2}(-1)^{\lambda+L}(2L+1)(2l_1+1)(2l_2+1)(2l'_1+1)(2l'_2+1)$$

$$\times\begin{bmatrix}l_1 & l'_1 & \lambda\\ 0 & 0 & 0\end{bmatrix}\begin{bmatrix}l_2 & l'_2 & \lambda\\ 0 & 0 & 0\end{bmatrix}\begin{Bmatrix}l_1 & l'_1 & \lambda\\ l'_2 & l_2 & \lambda\end{Bmatrix}\begin{bmatrix}l_1 & l_2 & L\\ 0 & 0 & 0\end{bmatrix}\begin{bmatrix}l'_1 & l'_2 & L\\ 0 & 0 & 0\end{bmatrix}. \tag{A10}$$

Turning now to the AN theory of Sec. II B, we seek the FBA to the frame-transformed AN T matrix $\mathcal{T}^J_{vjl,v_0j_0l_0}$ of (23). We start with the BF-FN K-matrix elements $K^{\Lambda}_{ll_0}(R)$, which satisfy an integral equation identical in form to (A1). The corresponding T-matrix elements in the FBA (evaluated at a body energy $\frac{1}{2}k_b^2$) are

$$T^{\Lambda}_{ll_0}(R)=\frac{4i}{k_b}\int_0^{\infty}\hat{j}_l(k_br)V^{(\Lambda)}_{ll_0}(r;R)\hat{j}_{l_0}(k_br)dr\ . \quad \text{(A11)}$$

This matrix element can be simplified using Eq. (19), viz.,

$$T^{\Lambda}_{ll_0}(R)=4ik_b\sum_{\lambda}g_{\lambda}(l,l_0;\Lambda)R^B_{\lambda}(l,l_0;k_b)\ , \quad \text{(A12)}$$

where the angular-coupling coefficients of the body-frame FN theory $g_{\lambda}(l,l_0;\Lambda)$ are given by (20) and the "body" radial integral is defined as

$$R^B_{\lambda}(l,l_0;k_b)\equiv\int_0^{\infty}j_l(k_b,r)v_{\lambda}(r;R)j_{l_0}(k_br)r^2dr\ . \quad \text{(A13)}$$

When the radial and vibrational frame transformations are applied to (A12), we obtain the FBA to the AN frame-transformed T-matrix element,

$$\mathcal{T}^J_{vjl,v_0j_0l_0}=4ik_b\sum_{\lambda}f_{\lambda}(j,l;j_0,l_0;J)R^B_{\lambda}(v,l;v_0,l_0;k_b)\ , \quad \text{(A14)}$$

where

$$R^B_{\lambda}(v,l;v_0,l_0;k_b)=\int_0^{\infty}j_l(k_br)\langle\phi_v(R)\,|\,v_{\lambda}(r,R)\,|\,\phi_{v_0}(R)\rangle j_{l_0}(k_br)r^2dr\ . \quad \text{(A15)}$$

For a long-range potential we can use (A5) in (A15) to obtain an explicit form for the body radial integral, viz., for $l+l_0-s_{\lambda}+3>0$,

$$R^B_{\lambda}(v,l;v_0,l_0;k_b)=B_{\lambda}(v,v_0)\pi 2^{-s_{\lambda}}k_b^{s_{\lambda}-3}\frac{\Gamma(s_{\lambda}-1)\Gamma\left[\frac{l+l_0-s_{\lambda}+3}{2}\right]}{\Gamma\left[\frac{l-l_0+s_{\lambda}}{2}\right]\Gamma\left[\frac{l+l_0+s_{\lambda}+1}{2}\right]\Gamma\left[\frac{l-l_0+s_{\lambda}}{2}\right]}\ . \quad \text{(A16)}$$

For example, for the quadrupole term $v_2(r)\sim -q/r^3$ as $r\to\infty$, which dominates rotational excitation very near threshold, we have

$$R^B_{\lambda}(v,l;v_0,l_0;k_b)=B_{\lambda}(v,v_0)\frac{\pi q}{8}\frac{\Gamma\left[\frac{l+l_0}{2}\right]}{\Gamma\left[\frac{l-l_0+3}{2}\right]\Gamma\left[\frac{l+l_0+4}{2}\right]\Gamma\left[\frac{l-l_0+3}{2}\right]} \quad \text{(A17)}$$

which is independent of the body-frame wave number k_b.

The AN-FBA differential cross section is

$$\frac{d\sigma}{d\Omega}(v_0,j_0\to v,j)=4\frac{k_b^2}{k_0^2}\sum_{\eta}C_{\eta}R^B_{\lambda}(v,l_1';v_0,l_1;k_b)\times R^B_{\lambda}(v,l_2';v_0,l_2;k_b)P_L(\cos\theta')\ . \quad \text{(A18)}$$

This differential cross section does not exhibit the correct behavior as $k_{vj}\to 0$ in the "conventional" AN theory, in which the choice $k_b=k_0$ is made. Hence in this case, Eq. (A18) is usually "corrected" by multiplication by the factor k_{vj}/k_0.

In the present implementation of the EMA (Sec. III C), we choose $k_b=(k_{vj}k_0)^{1/2}$, which automatically yields the factor k_{vj}/k_0 in (A18); no further *ad hoc* modification of this expression is necessary.

*Present address: Department of Mathematics, Rice University, Houston, TX 77001.

[1]M. Born and J. R. Oppenheimer, Ann. Phys. (Leipzig) 84, 457 (1927). For an introductory treatment, see M. A. Morrison, T. L. Estle, and N. F. Lane, *Quantum States of Atoms, Molecules, and Solids* (Prentice-Hall, Englewood Cliffs, New Jersey, 1976), Chap. 12. For a review, cf. W. Kolos, Adv. Quant. Chem. 5, 99 (1971).

[2]See M. A. Morrison and P. J. Hay, Phys. Rev. A 20, 740 (1979) for a discussion of adiabatic polarization potentials in electron-molecule scattering and R. A. Eades, D. A. Dixon, and D. G. Truhlar, J. Phys. B 15, 3365 (1982) for application to electron-atom collisions.

[3]For a qualitative introduction to the theory of electron-molecule scattering, see M. A. Morrison, Aust. J. Phys. 36, 239 (1983). The Appendix of this paper contains an annotated list of recent review articles at a higher level.

[4]For a thorough critical review of electron-molecule scattering theory through 1980, see N. F. Lane, Rev. Mod. Phys. 52, 29 (1980).

[5]D. W. Norcross and L. A. Collins, Adv. At. Mol. Phys. 18, 34 (1982).

[6]See Sec. IV of the review by D. E. Golden, N. F. Lane, A. Temkin, and E. Gerjuoy, Rev. Mod. Phys. 43, 642 (1971).

[7]D. M. Chase, Phys. Rev. 104, 838 (1956).

[8]Yu.D. Oksyuk, Zh. Eksp. Teor. Fiz. 49, 1261 (1965) [Sov.

Phys.—JETP 22, 873 (1966)].
[9]A. Temkin and K. V. Vasavada, Phys. Rev. 160, 109 (1967).
[10]S. Hara, J. Phys. Soc. Jpn. 27, 1593 (1969).
[11]E. S. Chang and A. Temkin, Phys. Rev. Lett. 23, 399 (1969).
[12]R. A. Abram and A. Herzenberg, Chem. Phys. Lett. 3, 198 (1969).
[13]A. Temkin, K. V. Vasavada, E. S. Chang, and A. Silver, Phys. Rev. 186, 57 (1969).
[14]E. S. Chang and A. Temkin, J. Phys. Soc. Jpn. 29, 172 (1970).
[15]A. Temkin and F. H. M. Faisal, Phys. Rev. A 3, 520 (1971).
[16]F. H. M. Faisal and A. Temkin, Phys. Rev. Lett. 28, 203 (1972).
[17]R. J. W. Henry and E. S. Chang, Phys. Rev. A 5, 276 (1972); see also E. S. Chang, Phys. Rev. Lett. 33, 1644 (1974).
[18]M. Shugard and A. Hazi, Phys. Rev. A 12, 1895 (1975).
[19]G. F. Drukarev, Zh. Eksp. Teor. Fiz. 67, 38 (1974) [Sov. Phys.—JETP 40, 18 (1975)].
[20]G. F. Drukarev and I. Y. Yurova, J. Phys. B 10, 355 (1977).
[21]A. Klonover and U. Kaldor, J. Phys. B 12, L61 (1979).
[22]I. Shimamura, Chem. Phys. Lett. 73, 328 (1980).
[23]I. Shimamura, Phys. Rev. A 23, 3350 (1981).
[24]D. W. Norcross, Phys. Rev. A 25, 764 (1982).
[25]I. Shimamura, *Symposium on Electron-Molecule Collisions, University of Tokyo, 1979,* edited by I. Shimamura and M. Matsuzawa (University of Tokyo, Tokyo, 1979), p. 13.
[26]D. W. Norcross and N. T. Padial, Phys. Rev. A 25, 226 (1982); see also L. A. Collins and D. W. Norcross, *ibid.* 18, 467 (1978) and references therein.
[27]R. J. W. Henry, Comput. Phys. Commun. 10, 375 (1975).
[28]B. M. Choi and R. T. Poe, Phys. Rev. A 16, 182 (1977); *ibid.* 16, 1831 (1977).
[29]W. Domcke, L. S. Cederbaum, and F. Kaspar, J. Phys. B 12, L359 (1979).
[30]E. F. Varracchio, Lett. Nuovo Cimento 24, 387 (1979); J. Phys. B 14, L511 (1981).
[31]N. Chandra, J. Phys. B 8, 1338 (1975).
[32]R. K. Nesbet, Phys. Rev. A 16, 1831 (1977).
[33]M. A. Morrison and N. F. Lane, Chem. Phys. Lett. 66, 527 (1979).
[34]A. M. Arthurs and A. Dalgarno, Proc. Roy. Soc. London Ser. A 256, 540 (1960).
[35]O. H. Crawford and A. Dalgarno, J. Phys. B 4, 494 (1971).
[36]N. F. Lane and S. Geltman, Phys. Rev. 160, 53 (1967).
[37]R. J. W. Henry and N. F. Lane, Phys. Rev. 183, 221 (1969).
[38]Cf. B. I. Schneider, Phys. Rev. A 11, 1957; D. A. Levin, A. W. Fliflet, and B. V. McKoy, *ibid.* 21, 1 1202 (1980); D. K. Watson, R. R. Lucchese, and T. N. Rescigno, *ibid.* 21, 738 (1980); T. N. Rescigno, A. E. Orel, A. U. Hazi, and B. V. McKoy, *ibid.* 26, 690 (1982).
[39]A preliminary report on this problem has appeared in A. Feldt and M. A. Morrison, J. Phys. B 15, 301 (1982). See Sec. III for remarks on the differences between these two investigations.
[40]Cf. R. W. Crompton, Adv. Electron. Electron Phys. 27, 1 (1969).
[41]In atomic units, $\hbar=m_e=a_0=e=1$. The unit of energy is $\hbar^2/m_e a_0^2=1E_h=2$ Ry$=27.212$ eV. The unit of distance is the first Bohr radius, $a_0=1$ bohr$=0.529\,18\times10^{-10}$ m. Cross sections are measured in units of squared 1 bohr, $a_0^2=0.29\times10^{-20}$ cm^2.
[42]L. Castillejo, I. C. Percival, and M. J. Seaton, Proc. Roy. Soc. London, Ser. A 254, 259 (1960).
[43]Primed coordinates will be used for the angular coordinates of the scattering electron in the space-fixed reference frame and unprimed coordinates in the body-fixed frame. Since the radial coordinate is unaffected by the rotation that relates these reference frames, r will be used in both.
[44]Cf. M. A. Morrison and L. A. Collins, Phys. Rev. A 23, 127 (1981) and references therein.
[45]M. E. Rose, *Elementary Theory of Angular Momentum* (Wiley, New York, 1957).
[46]M. A. Morrison, Comput. Phys. Commun. 21, 63 (1980).
[47]L. A. Collins, D. W. Norcross, and G. B. Schmid, Comput, Phys. Commun. 21, 79 (1980).
[48]A semicolon in an argument connotes *parametric* dependence on all variables following the semicolon.
[49]At all but near-threshold energies (where the FBA is applicable), numerous K-matrix elements contribute to the T-matrix elements for a particular nuclear excitation, $v_0j_0\rightarrow vj$ [cf. Eqs. (21) and discussion]. Therefore *primes* are used on the indices of K-matrix elements rather than, for example, vjl and $v_0j_0l_0$.
[50]E. S. Chang and U. Fano, Phys. Rev. A 6, 173 (1972).
[51]Cf. R. G. Newton, *Scattering Theory of Waves and Particles,* 2nd ed. (Springer, New York, 1982), Chap. 16.
[52]For collisions with a molecule in a Σ electronic state, the quantum numbers corresponding to $\hat{l}\cdot\hat{R}$ and $\hat{J}\cdot\hat{R}$ are identical (Λ). See B. R. Judd, *Angular Momentum Theory for Diatomic Molecules* (Academic, New York, 1975).
[53]For $\Lambda=0$ the rotational functions are just the spherical harmonics $Y_{JM}(\hat{R})$.
[54]Cf. A. S. Davydov, *Quantum Mechanics,* 2nd ed. (Pergamon, New York, 1976), Chap. V.
[55]Cf. E. Merzbacher, *Quantum Mechanics,* 2nd ed. (Wiley, New York, 1970), Chap. 16.
[56]J. N. Bardsley and R. K. Nesbet, Phys. Rev. A 8, 203 (1973).
[57]See also E. S. Chang, J. Phys. B 14, 893 (1981) and references therein; R. K. Nesbet, J. Phys. B 13, L193 (1980); E. S. Chang, Phys. Rev. A 2, 1403 (1970).
[58]I. I. Fabrikant, J. Phys. B 14, 335 (1981).
[59](a) E. Gerjuoy and S. Stein, Phys. Rev. 97, 1671 (1955); (b) A. Dalgarno and R. J. Moffett, Proc. Natl. Acad. Sci. India A 33, 511 (1963).
[60]In conventional AN theory, threshold is approached as $k_0\rightarrow k_{vj}$, not $k_b\rightarrow0$. For small threshold energies, this distinction is not germane to the present argument. In the EMA of Sec. II D the approach to threshold is $k_b\rightarrow0$.
[61]W. W. Bell, *Special Functions for Scientists and Engineers* (Van Nostrand, New York, 1968), Chap. 2.
[62]J. R. Taylor, *Scattering Theory* (Wiley, New York, 1972).
[63]A. N. Feldt and M. A. Morrison, Phys. Rev. A 29, 401 (1984).
[64]For a review of approximations to the static potential, see D. G. Truhlar, in *Chemical Applications of Atomic and Molecular Electrostatic Potentials,* edited by P. Politzer and D. G. Truhlar (Plenum, New York, 1981), p. 123.
[65]Cf. Henry F. Schaefer III, *The Electronic Structure of Atoms and Molecules* (Addison-Wesley, Reading, Mass., 1972).
[66]J. W. Moskowitz and L. C. Snyder, in *Methods of Electronic Structure Theory,* edited by H. F. Schaeffer III (Plenum, New York, 1977), p. 387.
[67]W. Kolos and C. C. J. Roothaan, Rev. Mod. Phys. 32, 219 (1980).
[68]W. Kolos and L. Wolniewicz, J. Chem. Phys. 49, 404 (1968).
[69]W. R. G. Barnes, P. J. Bray, and N. F. Ramsey, Phys. Rev. 94, 893 (1954).
[70]N. J. Marrick and N. J. Ramsey, Phys. Rev. 88, 228 (1952).
[71]N. F. Ramsey, Phys. Rev. 88, 1075 (1982).
[72]Using our basis set to generate ground-state electronic wave

functions for H_2 at nonequilibrium values of R, extracting from these $q(R)$, and averaging this quantity over the ground-vibrational-state wave function (obtained by numerically solving the nuclear Schrödinger equation), we obtain $0.4705ea_0^2$.

[73]J. D. Poll and L. Wolniewicz, J. Chem. Phys. 68, 3053 (1978).

[74]M. A. Morrison, N. F. Lane, and L. A. Collins, Phys. Rev. A 15, 2186 (1977).

[75]S. Hara, J. Phys. Soc. Jpn. 22, 710 (1967).

[76]M. A. Morrison and L. A. Collins, Phys. Rev. A 17, 918 (1978).

[77]W. E. Weitzel III, T. L. Gibson, and M. A. Morrison, Comput. Phys. Commun. 30, 151 (1983).

[78]T. L. Gibson and M. A. Morrison, J. Phys. B 15, L221 (1982).

[79]The eigenphase shifts are obtained by diagonalizing the K matrix and taking the arctangent of the resulting eigenvalues. The eigenphase sum in, for example, the BF-FN formulation, is obtained for each electron-molecule symmetry by summing the corresponding eigenphase shifts.

[80]L. A. Collins, W. D. Robb, and M. A. Morrison, Phys. Rev. A 21, 488 (1980).

[81]See, however, B. I. Schneider and L. A. Collins, Phys. Rev. A 27, 2847 (1983), and references therein for more rigorous treatments of polarization effects.

[82]N. F. Lane and R. J. W. Henry, Phys. Rev. 173, 183 (1968).

[83]T. L. Gibson and M. A. Morrison, J. Phys. B 15, L221 (1982); Phys. Rev. A (to be published).

[84]A. Temkin, Phys. Rev. 107, 1004 (1957).

[85]M. A. Morrison, in *Electron-Molecule and Photon-Molecule Collisions,* edited by T. N. Rescigno, B. V. McKoy, and B. I. Schneider (Plenum, New York, 1979), p. 15.

[86]See Eqs. (19) and (20) of Ref. 34.

[87]U. Fano and D. Dill, Phys. Rev. A 6, 185 (1972).

[88]Additional useful forms can be found in Appendix B of Ref. 26, in the Appendix to Ref. 72, and in the Appendix of N. Chandra, Phys. Rev. A 16, 80 (1977).

[89]To some extent, this agreement is fortuitous. The rigid-rotor approximation yields cross sections that are smaller than those obtained when vibrational effects are included (cf. Refs. 21 and 37). The error thereby introduced is partially canceled by that due to use of a FEG exchange potential that was tuned in the Σ_g symmetry.

[90]R. W. Crompton, D. K. Gibson, and A. I. McIntoch, Aust. J. Phys. 22, 715 (1969), and references therein.

[91]I. S. Gradshteyn and I. M. Ryzhik, *Tables of Integrals, Series, and Products,* 2nd ed. (Academic, New York, 1980).

[92]A. N. Feldt, T. L. Gibson, and M. A. Morrison, Bull. Am. Phys. Soc. 28, 811 (1983).